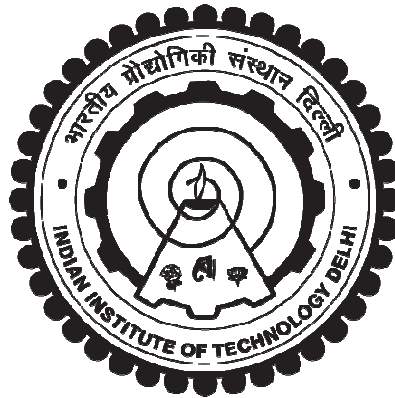


**DESIGN AND DEVELOPMENT OF IMPROVED POWER
QUALITY CONVERTERS FED PERMANENT MAGNET
BRUSHLESS DC MOTOR DRIVES**

VASHIST BIST



**DEPARTMENT OF ELECTRICAL ENGINEERING
INDIAN INSTITUTE OF TECHNOLOGY DELHI
HAUZ KHAS, NEW DELHI – 110016, INDIA
APRIL 2015**

© Indian Institute of Technology Delhi (IITD), New Delhi, 2015

**DESIGN AND DEVELOPMENT OF IMPROVED POWER
QUALITY CONVERTERS FED PERMANENT MAGNET
BRUSHLESS DC MOTOR DRIVES**

by

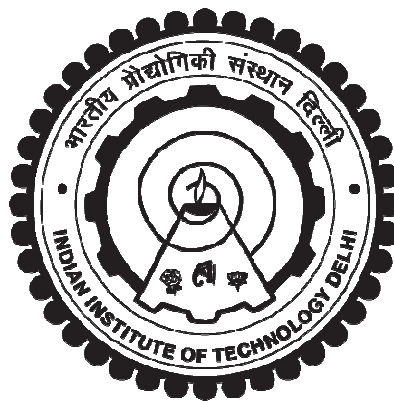
VASHIST BIST
Electrical Engineering Department

Submitted

in fulfillment of the requirements of the degree of

DOCTOR OF PHILOSOPHY

to the



INDIAN INSTITUTE OF TECHNOLOGY DELHI

APRIL 2015

CERTIFICATE

It is certified that the thesis entitled “**Design and Development of Improved Power Quality Converters fed Permanent Magnet Brushless DC Motor Drives,**” being submitted by **Mr. Vashist Bist** for award of the degree of **Doctor of Philosophy** in the Department of Electrical Engineering, Indian Institute of Technology Delhi, is a record of the student work carried out by him under my supervision and guidance. The matter embodied in this thesis has not been submitted for award of any other degree or diploma.

Dated: April 06, 2015

(Prof. Bhim Singh)

**Electrical Engineering Department,
Indian Institute of Technology Delhi,
Hauz Khas, New Delhi-110016, India.**

ACKNOWLEDGEMENTS

I wish to express my deepest gratitude and indebtedness to **Prof. Bhim Singh** for providing me an opportunity to carry out the Ph.D. work under his supervision. His keenness and vision have played an important role in guiding me throughout this study. Working under him has been a wonderful experience, which has provided a deep insight to the world of research. Determination, dedication, innovativeness, resourcefulness and discipline of **Prof. Bhim Singh** have been the inspiration for me to complete this work. His consistent encouragement, continuous monitoring and commitments to excellence have always motivated me to improve my work and use the best of my capabilities.

My sincere thanks and deep gratitude are to **Prof. T.S. Bhatti, Prof. G. Bhuvaneswari,** and **Prof. Sukumar Mishra**, all SRC members for their valuable guidance and consistent support during my research work.

I wish to convey my sincere thanks to **Prof. Bhim Singh, Prof. B. P. Singh, Prof. S. S. Murthy, Prof. M. Hanmandlu, Prof. G. Bhuvaneswari, Prof. Subrat Kar, Dr. Mashuq un Nabi** and **Dr. S. Janardhanan** for their valuable inputs during my course work which helped me to enrich my knowledge. I am grateful to IIT Delhi for providing me the research facilities. I would wish to express my sincere gratitude to **Prof. K. R. Rajagopal**, Prof. in-charge, PG Machine Lab., for providing me immense facilities to carry out experimental work. I am too grateful to **Prof. G. Bhuvaneswari**, Prof. in-charge, Power Electronics Lab for her whole hearted support in my research work. Thanks are due to Sh. Gurcharan Singh, Sh. Dhan Raj Singh, Sh. Srichand, Sh. Puran Singh, Sh. Jagbir Singh, Sh. Satey Singh Negi of PG Machines Lab, UG Machines Lab and Power Electronics Lab., IIT Delhi for providing me the facilities and assistance during this work.

I would like to offer my sincere thanks to Dr. Sanjeev Singh, Dr. Shailendra Sharma and Dr. Ashish Shrivastava who have endorsed me during initial start-up of my research work. I too would wish to thank Dr. Sandeep V., Dr. Rajashekhar Reddy, Dr. Sabharaj Arya, Dr. Shikha Singh, Dr. Rajesh Mutharath, Mr. Raj Kumar Garg, Mr. Ram Niwas, Mr. Arun Kumar Verma, Ms. Swati Narula, Mr. Aman Jha, Mr. Saurabh Mangalik, Mr. Sangram Keshri Nayak, Mr. Narendra Singh, Mr. Rahul Pandey, Mr. Rajan Kumar Sonkar and Mr. Ikhlq Bohru for their valuable aid and co-operation. My sincere thanks are due to Mr. Madishetti Sandeep, Mr. N K Swami Naidu and Mr. Chinmay Jain for co-operation and informal support in pursuing experimental work. How could I forget my hostel mates Mr. Anup Kumar Mandpura and Mr. Somesh Bhattacharya, who supported and inspired me during my stay in 'Jwalamukhi' hostel. I am likewise thankful to those who suffer directly or indirectly helped me to finish my dissertation study.

Blessings of my father, Late Sh. M. S. Bisht have always strengthened me in my entire life. My richest love, appreciation and indebtedness go to my mother, Mrs. Savita Bisht for her dreams, sacrifices and wholeheartedly endorses. Her trust and trust in my capabilities have always motivated me to reach higher academic degrees. I must appreciate my sister, Ms. Vaishali Bisht for handling family responsibilities in my absence and her kind support.

At last, I am beholden to almighty for their blessings to help me to raise my academic level to this stage. I pray for their benediction in my future endeavors. Their blessings may be showered on me for strength, wisdom and determination to achieve in future.

Date: April 06, 2015

Vashist Bist

ABSTRACT

Energy efficiency and cost reduction in the development of permanent magnet brushless DC (PMBLDC) motor drives have gained importance due to their advantageous features over existing motors. High efficiency, high power density, compact size, silent operation, high reliability and low wear and tear of the PMBLDC motor, makes it a suitable choice in many low and medium power applications. Due to these features, PMBLDC motors are widely used in household equipments, industrial tools, heating, ventilation and air conditioning (HVAC), robotics, automation and medical applications.

This research work aims at the development of the power factor correction converters for feeding PMBLDC motor drives as a cost effective solution for low power household appliances. The PMBLDC motor requires a three phase voltage source inverter (VSI) for achieving an electronic commutation based on rotor position as sensed by Hall-Effect position sensors. This PMBLDC motor drive is driven by single phase AC supply via an uncontrolled diode bridge rectifier (DBR) and high value of DC bus capacitor. Such combination draws peaky current from the supply system, which is rich in harmonics and has very high total harmonic distortion (THD) of supply current at AC mains. This leads high crest factor (CF) of the supply current and very low power factor (PF) at AC mains. Such power quality indices are not acceptable within the limit of IEC 61000-3-2. Hence, single phase PFC converters are used to improve the power quality of PMBLDC motor drive at AC mains.

The selection of suitable PFC converter for particular application depends upon various aspects such as total number of components of PFC converter, voltage and power rating of BLDC motor, requirement of galvanic isolation, cost and efficiency of the overall system. There are many available configurations of the PFC converters, which are classified into five different

categories of non-isolated PFC converters, bridgeless non-isolated PFC converters, isolated PFC converters, bridgeless isolated PFC converters and integrated and high quality rectifiers. Among them, the bridgeless configurations are designed for reducing the conduction losses in the front end PFC converter by partial elimination of the diode bridge rectifier. Moreover, the control strategy of the PFC converter also plays a vital role in deciding the performance and cost of the overall system. In this work, PFC converter operating in discontinuous conduction mode (DCM) is used to control the PFC converter via an approach of voltage follower; which requires a single voltage sensor for PFC and DC link voltage control.

Analysis, design and control of buck-boost PFC converters for improvements in power quality at AC mains of the PMBLDC motor drive is presented in this work. The other major aspect of the work includes simplicity in control, reducing the number of sensors and cost and increasing the overall efficiency of the system. Many new configurations of single phase PFC converters are presented in this work for feeding the PMBLDC motor drive. Moreover, the speed of PMBLDC motor is controlled by adjusting the DC link voltage of the VSI feeding PMBLDC motor. This allows the VSI to operate in fundamental frequency switching for reducing the switching losses in VSI.

Moreover, a new sensorless control scheme of PMBLDC motor is also developed to operate it with variable DC link voltage control method of speed control of PMBLDC motor. A two step starting method of PMBLDC motor drive is also proposed for satisfactory starting of PMBLDC motor at rated loading conditions. The performance of these PFC based PMBLDC motor drives are validated on the models developed in MATLAB/Simulink environment. Moreover, the performance of selected configurations of PFC converters feeding PMBLDC motor drives is also verified experimentally on a developed hardware prototype. This performance evaluation

includes the steady state performances at various speeds and dynamic performance during starting, speed control, loading of PMBLDC motor and supply voltage fluctuations at AC mains. The steady state performance also includes the voltage and current waveforms of various components (semiconductors, magnetic and capacitive) of PFC converters for selection criteria of these components. An acceptable power quality indices of these PFC converters fed PMBLDC motor drives are also evaluated at AC mains. These power quality indices are found within the acceptable limits of international power quality standard IEC 61000-3-2.

TABLE OF CONTENTS

	Page No.
Certificate	i
Acknowledgements	ii
Abstract	iv
Table of Contents	vii
List of Figures	xxvii
List of Tables	lxv
List of Abbreviations	lxviii
List of Symbols	lxx
CHAPTER I INTRODUCTION	1-11
1.1 General	1
1.2 State of Art on Permanent Magnet Brushless DC Motors	2
1.2.1 Development of BLDC Motors	2
1.2.2 Control of BLDC Motors	3
1.2.3 Application Potential of BLDC Motors	3
1.3 Power Quality Issues in Brushless DC Motor Drives	4
1.3.1 Power Quality Issues in a DBR fed BLDC Motor Drives	4
1.3.2 Power Quality Standards and Power Quality Indices	5
1.3.3 Power Quality Improvements in PFC Converters fed BLDC Motor Drives	5
1.4 Scope of Work	6
1.4.1 Analysis, Design and Development of BLDC Motor Drives	6
1.4.2 Analysis, Design and Development of PFC Converters Feeding BLDC Motor Drives	6
1.4.3 Analysis, Design and Development of PFC Converters Feeding Sensorless BLDC Motor Drives	8
1.5 Outlines of Chapters	9
CHAPTER II LITERATURE REVIEW	12-29
2.1 General	12

2.2	Literature Survey	13
2.2.1	Review of BLDC Motor Drives	13
2.2.3	Review of Sensorless Control of BLDC Motor Drives	15
2.2.3	Review of PFC Converters	17
2.2.3	Review of PFC Converters Feeding BLDC Motor Drives	25
2.3	Identified Research Areas	27
2.4	Conclusions	29

CHAPTER III CLASSIFICATION AND CONFIGURATIONS OF PFC CONVERTERS FED BLDC MOTOR DRIVES 30-44

3.1	General	30
3.2	Requirements of PFC Converters for Feeding BLDC Motor Drives	30
3.3	Classification of PFC Converters Fed BLDC Motor Drives	32
3.4	Configurations of PFC Converters For BLDC Motor Drives	33
3.4.1	Non-Isolated PFC Converters Fed BLDC Motor Drives	34
3.4.2	Bridgeless Non-Isolated PFC Converters Fed BLDC Motor Drives	36
3.4.3	Isolated PFC Converters Fed BLDC Motor Drives	38
3.4.4	Bridgeless Isolated PFC Converters Fed BLDC Motor Drives	39
3.4.5	Integrated and High Quality Rectifiers Fed BLDC Motor Drives	40
3.5	Comparative Features of Various PFC Converters Based on Application of BLDC Motor Drives	43
3.6	Conclusions	43

CHAPTER IV DESIGN, MODELING AND IMPLEMENTATION OF BLDC MOTOR DRIVES 45-101

4.1	General	45
4.2	Circuit Configurations of BLDC Motor Drives	46
4.2.1	A DBR fed BLDC Motor Drive	46
4.2.2	A PFC Converter fed BLDC Motor Drive with Constant DC Link Voltage of VSI	46
4.2.2.1	PFC Converter Operating in CCM	47
4.2.2.2	PFC Converter Operating in DCM	48
4.2.3	A PFC Converter fed BLDC Motor Drive with Variable DC Link Voltage of VSI	48

4.2.3.1	PFC Converter Operating in CCM	49
4.2.3.2	PFC Converter Operating in DCM	49
4.3	Design of Various Configurations of BLDC Motor Drives	51
4.3.1	A DBR Fed BLDC Motor Drive	51
4.3.2	A PFC Converter fed BLDC Motor Drive with Constant DC Link Voltage of VSI	52
4.3.2.1	PFC Converter Operating in CCM	52
4.3.2.2	PFC Converter Operating in DCM	54
4.3.3	A PFC Converter fed BLDC Motor Drive with Variable DC Link Voltage of VSI	55
4.3.3.1	PFC Converter Operating in CCM	55
4.3.3.2	PFC Converter Operating in DCM	56
4.4	Modes of Operation of BLDC Motor Drives	58
4.4.1	PWM Based Control of BLDC Motor Drives	58
4.4.2	FFS Based Control of BLDC Motor Drives (120 ⁰ Conduction Mode)	58
4.5	Control of BLDC Motor Drives	60
4.5.1	DBR Fed BLDC Motor Drive	60
4.5.1.1	Speed Controller	61
4.5.1.2	Reference Current Generator	62
4.5.1.3	PWM Current Controller	62
4.5.2	PFC Converter fed BLDC Motor Drive with Constant DC Link Voltage of VSI	63
4.5.2.1	PFC Converter Operating in CCM	63
4.5.2.2	PFC Converter Operating in DCM	64
4.5.3	PFC Converter fed BLDC Motor Drive with Variable DC Link Voltage of VSI	65
4.5.3.1	PFC Converter Operating in CCM	66
4.5.3.2	PFC Converter Operating in DCM	67
4.6	Modeling of BLDC Motor Drives	68
4.7	MATLAB Based Modeling and Simulation of BLDC Motor Drives	72
4.8	Hardware Implementation of BLDC Motor Drives	73
4.8.1	Hardware Implementation of DBR fed BLDC Motor Drive	74
4.8.1.1	Development of Isolation and Amplification Circuit for PWM Signals	74
4.8.1.2	Development of Signal Conditioning Circuit for Voltage Sensors	74

4.8.1.3	Development of Signal Conditioning Circuit for Current Sensors	75
4.8.1.4	Development of Control Algorithm on Digital Signal Processor	76
4.8.2	Hardware Implementation of PFC Converter Fed BLDC Motor Drive with Constant DC Link Voltage of VSI	77
4.8.3	Hardware Implementation of PFC Converter Fed BLDC Motor Drive with Variable DC Link Voltage of VSI	78
4.9	Results and Discussion	79
4.9.1	Performance of DBR fed BLDC Motor Drive	79
4.9.1.1	Steady State Performance	79
4.9.1.2	Dynamic Performance During Starting and Speed Control	79
4.9.1.3	Dynamic Performance Under Load Variation	81
4.9.1.4	Power Quality Performance at Variable Speeds	82
4.9.2	Performance of PFC Converter Fed BLDC Motor Drive with Constant DC Link Voltage of VSI	84
4.9.2.1	Steady State Performance	84
4.9.2.2	Dynamic Performance During Starting and Speed Control	85
4.9.2.3	Dynamic Performance Under Load Variation and Supply Voltage Fluctuation	85
4.9.2.4	Power Quality Performance at Variable Speeds and Different Supply Voltages	87
4.9.3	Performance of PFC Converter Fed BLDC Motor Drive with Variable DC Link Voltage of VSI	90
4.9.3.1	Steady State Performance	90
4.9.3.2	Dynamic Performance During Starting and Speed Control	92
4.9.3.3	Dynamic Performance Under Load Variation and Supply Voltage Fluctuation	92
4.9.3.4	Power Quality Performance at Variable Speeds and Different Supply Voltages	94
4.10	Comparative Evaluation of Various Configurations of BLDC Motor Drives	96
4.10.1	Comparison on the Basis of Improved Power Quality Operation	97
4.10.2	Comparison on the Basis of Losses and Efficiency	98
4.10.3	Comparison on the Basis of Control Complexity	98
4.10.4	Comparison on the Basis of Sensor Requirements and Cost	99
4.11	Conclusions	101

CHAPTER V DESIGN, MODELING AND IMPLEMENTATION OF NON-ISOLATED PFC CONVERTERS FED BLDC MOTOR DRIVES 102-202

5.1	General	102
5.2	Classification of Non-Isolated PFC Converters Fed BLDC Motor Drives	102
5.3	Configurations and Operating Principle of Non-Isolated PFC Converters Fed BLDC Motor Drives	103
5.3.1	Non-Isolated PFC Buck-Boost Converter Fed BLDC Motor Drive	103
5.3.2	Non-Isolated PFC Cuk Converter Fed BLDC Motor Drive	105
5.3.3	Non-Isolated PFC SEPIC Fed BLDC Motor Drive	107
5.3.4	Non-Isolated PFC Zeta Converter Fed BLDC Motor Drive	110
5.3.5	Non-Isolated PFC Luo Converter Fed BLDC Motor Drive	112
5.3.6	Non-Isolated PFC CSC Converter Fed BLDC Motor Drive	114
5.3.7	Non-Isolated PFC Sheppard-Taylor Converter Fed BLDC Motor Drive	116
5.3.8	Non-Isolated PFC Switched-Capacitor Buck-Boost Converter Fed BLDC Motor Drive	118
5.4	Design of Non-Isolated PFC Converters Fed BLDC Motor Drives	120
5.4.1	Non-Isolated PFC Buck-Boost Converter Fed BLDC Motor Drive	123
5.4.2	Non-Isolated PFC Cuk Converter Fed BLDC Motor Drive	124
5.4.3	Non-Isolated PFC SEPIC Fed BLDC Motor Drive	127
5.4.4	Non-Isolated PFC Zeta Converter Fed BLDC Motor Drive	129
5.4.5	Non-Isolated PFC Luo Converter Fed BLDC Motor Drive	131
5.4.6	Non-Isolated PFC CSC Converter Fed BLDC Motor Drive	133
5.4.7	Non-Isolated PFC Sheppard-Taylor Converter Fed BLDC Motor Drive	135
5.4.8	Non-Isolated PFC Switched-Capacitor Buck-Boost Converter Fed BLDC Motor Drive	137
5.5	Control of Non-Isolated PFC Converters Fed BLDC Motor Drives	138
5.6	MATLAB Based Modeling and Simulation of Non-Isolated PFC Converters Fed BLDC Motor Drives	140
5.7	Hardware Implementation of Non-Isolated PFC Converters Fed BLDC Motor Drives	141
5.8	Results and Discussion	141
5.8.1	Performance of Non-Isolated PFC Buck-Boost Converter Fed BLDC Motor Drive	141
5.8.1.1	Steady State Performance	141
5.8.1.2	Dynamic Performance During Starting and Speed Control	143

5.8.1.3	Dynamic Performance Under Load Variation and Supply Voltage Fluctuation	145
5.8.1.4	Power Quality Performance at Variable Speeds and Different Supply Voltages	146
5.8.2	Performance of Non-Isolated PFC Cuk Converter Fed BLDC Motor Drive	149
5.8.2.1	Steady State Performance	149
5.8.2.2	Dynamic Performance During Starting and Speed Control	151
5.8.2.3	Dynamic Performance Under Load Variation and Supply Voltage Fluctuation	153
5.8.2.4	Power Quality Performance at Variable Speeds and Different Supply Voltages	154
5.8.3	Performance of Non-Isolated PFC SEPIC Fed BLDC Motor Drive	157
5.8.3.1	Steady State Performance	157
5.8.3.2	Dynamic Performance During Starting and Speed Control	159
5.8.3.3	Dynamic Performance Under Load Variation and Supply Voltage Fluctuation	161
5.8.3.4	Power Quality Performance at Variable Speeds and Different Supply Voltages	162
5.8.4	Performance of Non-Isolated PFC Zeta Converter Fed BLDC Motor Drive	165
5.8.4.1	Steady State Performance	165
5.8.4.2	Dynamic Performance During Starting and Speed Control	167
5.8.4.3	Dynamic Performance Under Load Variation and Supply Voltage Fluctuation	169
5.8.4.4	Power Quality Performance at Variable Speeds and Different Supply Voltages	170
5.8.5	Performance of Non-Isolated PFC Luo Converter Fed BLDC Motor Drive	173
5.8.5.1	Steady State Performance	173
5.8.5.2	Dynamic Performance During Starting and Speed Control	175
5.8.5.3	Dynamic Performance Under Load Variation and Supply Voltage Fluctuation	177
5.8.5.4	Power Quality Performance at Variable Speeds and Different Supply Voltages	178
5.8.6	Performance of Non-Isolated PFC CSC Converter Fed BLDC Motor Drive	181
5.8.6.1	Steady State Performance	181

5.8.6.2	Dynamic Performance During Starting and Speed Control	183
5.8.6.3	Dynamic Performance Under Load Variation and Supply Voltage Fluctuation	185
5.8.6.4	Power Quality Performance at Variable Speeds and Different Supply Voltages	186
5.8.7	Performance of Non-Isolated PFC Sheppard Taylor Converter Fed BLDC Motor Drive	189
5.8.7.1	Steady State Performance	189
5.8.7.2	Dynamic Performance During Starting and Speed Control	190
5.8.7.3	Dynamic Performance Under Load Variation and Supply Voltage Fluctuation	191
5.8.7.4	Power Quality Performance at Variable Speeds and Different Supply Voltages	191
5.8.8	Performance of Non-Isolated PFC Switched-Capacitor Buck-Boost Converter Fed BLDC Motor Drive	193
5.8.8.1	Steady State Performance	193
5.8.8.2	Dynamic Performance During Starting and Speed Control	194
5.8.8.3	Dynamic Performance Under Load Variation and Supply Voltage Fluctuation	195
5.8.8.4	Power Quality Performance at Variable Speeds and Different Supply Voltages	195
5.9	Comparative Evaluation of Various Non-Isolated PFC Converters Fed BLDC Motor Drives	197
5.9.1	Comparison on the Basis of Number of Components of PFC Converter	197
5.9.2	Comparison on the Basis of Improved Power Quality Operation	198
5.9.3	Comparison on the Basis of Stress on PFC Converter Switches	200
5.9.4	Comparison on the Basis of Application Potential and EMI Issues	201
5.10	Conclusions	202

CHAPTER VI DESIGN, MODELING AND IMPLEMENTATION OF BRIDGELESS NON-ISOLATED PFC CONVERTERS FED BLDC MOTOR DRIVES 203-313

6.1	General	203
6.2	Classification of Bridgeless Non-Isolated PFC Converters Fed BLDC Motor Drives	203
6.3	Configurations and Operating Principle of Bridgeless Non-Isolated PFC Converters Fed BLDC Motor Drives	204

6.3.1	Bridgeless Non-Isolated PFC Buck-Boost Converter Fed BLDC Motor Drive	204
6.3.2	Bridgeless Non-Isolated PFC Cuk Converter Fed BLDC Motor Drive	207
6.3.3	Bridgeless Non-Isolated PFC SEPIC Fed BLDC Motor Drive	210
6.3.4	Bridgeless Non-Isolated PFC Zeta Converter Fed BLDC Motor Drive	213
6.3.5	Bridgeless Non-Isolated PFC Luo Converter Fed BLDC Motor Drive	216
6.3.6	Bridgeless Non-Isolated PFC CSC Converter Fed BLDC Motor Drive	219
6.3.7	Bridgeless Non-Isolated PFC Sheppard Taylor Converter Fed BLDC Motor Drive	222
6.3.8	Bridgeless Non-Isolated PFC Switched-Capacitor Buck-Boost Converter Fed BLDC Motor Drive	227
6.4	Design of Bridgeless Non-Isolated PFC Converters Fed BLDC Motor Drives	230
6.4.1	Bridgeless Non-Isolated PFC Buck-Boost Converter Fed BLDC Motor Drive	233
6.4.2	Bridgeless Non-Isolated PFC Cuk Converter Fed BLDC Motor Drive	234
6.4.3	Bridgeless Non-Isolated PFC SEPIC Fed BLDC Motor Drive	237
6.4.4	Bridgeless Non-Isolated PFC Zeta Converter Fed BLDC Motor Drive	239
6.4.5	Bridgeless Non-Isolated PFC Luo Converter Fed BLDC Motor Drive	241
6.4.6	Bridgeless Non-Isolated PFC CSC Converter Fed BLDC Motor Drive	243
6.4.7	Bridgeless Non-Isolated PFC Sheppard Taylor Converter Fed BLDC Motor Drive	245
6.4.8	Bridgeless Non-Isolated PFC Switched-Capacitor Buck-Boost Converter Fed BLDC Motor Drive	247
6.5	Control of Bridgeless Non-Isolated PFC Converters Fed BLDC Motor Drives	249
6.6	MATLAB Based Modeling and Simulation of Bridgeless Non-Isolated PFC Converters Fed BLDC Motor Drives	250
6.7	Hardware Implementation of Bridgeless Non-Isolated PFC Converters Fed BLDC Motor Drives	251
6.8	Results and Discussion	252
6.8.1	Performance of Bridgeless Non-Isolated PFC Buck-Boost Converter Fed BLDC Motor Drive	252
6.8.1.1	Steady State Performance	252
6.8.1.2	Dynamic Performance During Starting and Speed Control	254
6.8.1.3	Dynamic Performance Under Load Variation and Supply Voltage Fluctuation	256
6.8.1.4	Power Quality Performance at Variable Speeds and Different Supply Voltages	256

6.8.2	Performance of Bridgeless Non-Isolated PFC Cuk Converter Fed BLDC Motor Drive	260
6.8.2.1	Steady State Performance	260
6.8.2.2	Dynamic Performance During Starting and Speed Control	263
6.8.2.3	Dynamic Performance Under Load Variation and Supply Voltage Fluctuation	264
6.8.2.4	Power Quality Performance at Variable Speeds and Different Supply Voltages	266
6.8.3	Performance of Bridgeless Non-Isolated PFC SEPIC Fed BLDC Motor Drive	269
6.8.3.1	Steady State Performance	269
6.8.3.2	Dynamic Performance During Starting and Speed Control	271
6.8.3.3	Dynamic Performance Under Load Variation and Supply Voltage Fluctuation	273
6.8.3.4	Power Quality Performance at Variable Speeds and Different Supply Voltages	273
6.8.4	Performance of Bridgeless Non-Isolated PFC Zeta Converter Fed BLDC Motor Drive	277
6.8.4.1	Steady State Performance	277
6.8.4.2	Dynamic Performance During Starting and Speed Control	278
6.8.4.3	Dynamic Performance Under Load Variation and Supply Voltage Fluctuation	279
6.8.4.4	Power Quality Performance at Variable Speeds and Different Supply Voltages	280
6.8.5	Performance of Bridgeless Non-Isolated PFC Luo Converter Fed BLDC Motor Drive	282
6.8.5.1	Steady State Performance	282
6.8.5.2	Dynamic Performance During Starting and Speed Control	284
6.8.5.3	Dynamic Performance Under Load Variation and Supply Voltage Fluctuation	286
6.8.5.4	Power Quality Performance at Variable Speeds and Different Supply Voltages	286
6.8.6	Performance of Bridgeless Non-Isolated PFC CSC Converter Fed BLDC Motor Drive	290
6.8.6.1	Steady State Performance	290
6.8.6.2	Dynamic Performance During Starting and Speed Control	292
6.8.6.3	Dynamic Performance Under Load Variation and Supply Voltage Fluctuation	294

6.8.6.4	Power Quality Performance at Variable Speeds and Different Supply Voltages	295
6.8.7	Performance of Bridgeless Non-Isolated PFC Sheppard-Taylor Converter Fed BLDC Motor Drive	298
6.8.7.1	Steady State Performance	298
6.8.7.2	Dynamic Performance During Starting and Speed Control	300
6.8.7.3	Dynamic Performance Under Load Variation and Supply Voltage Fluctuation	300
6.8.7.4	Power Quality Performance at Variable Speeds and Different Supply Voltages	301
6.8.8	Performance of Bridgeless Non-Isolated PFC Switched-Capacitor Buck-Boost Converter Fed BLDC Motor Drive	303
6.8.8.1	Steady State Performance	303
6.8.8.2	Dynamic Performance During Starting and Speed Control	303
6.8.8.3	Dynamic Performance Under Load Variation and Supply Voltage Fluctuation	304
6.8.8.4	Power Quality Performance at Variable Speeds and Different Supply Voltages	305
6.9	Comparative Evaluation of Various Bridgeless Non-Isolated PFC Converters Fed BLDC Motor Drives	307
6.9.1	Comparison on the Basis of Number of Components of PFC Converter	307
6.9.2	Comparison on the Basis of Improved Power Quality Operation	308
6.9.3	Comparison on the Basis of Stress on PFC Converter Switches	309
6.9.4	Comparison on the Basis of Application Potential and EMI Issues	311
6.10	Conclusions	312
CHAPTER VII	DESIGN, MODELING AND IMPLEMENTATION OF ISOLATED PFC CONVERTERS FED BLDC MOTOR DRIVES	314-385
7.1	General	314
7.2	Classification of Isolated PFC Converters Fed BLDC Motor Drive	314
7.3	Configurations and Operating Principle of Isolated PFC Converters Fed BLDC Motor Drives	315
7.3.1	Isolated PFC Flyback Converter Fed BLDC Motor Drive	315
7.3.2	Isolated PFC Cuk Converter Fed BLDC Motor Drive	317
7.3.3	Isolated PFC SEPIC Fed BLDC Motor Drive	319

7.3.4	Isolated PFC Zeta Converter Fed BLDC Motor Drive	321
7.3.5	Isolated PFC Luo Converter Fed BLDC Motor Drive	323
7.3.6	Isolated PFC Sheppard-Taylor Converter Fed BLDC Motor Drive	325
7.4	Design of Isolated PFC Converters Fed BLDC Motor Drives	328
7.4.1	Isolated PFC Flyback Converter Fed BLDC Motor Drive	331
7.4.2	Isolated PFC Cuk Converter Fed BLDC Motor Drive	332
7.4.3	Isolated PFC SEPIC Fed BLDC Motor Drive	336
7.4.4	Isolated PFC Zeta Converter Fed BLDC Motor Drive	338
7.4.5	Isolated PFC Luo Converter Fed BLDC Motor Drive	339
7.4.6	Isolated PFC Sheppard-Taylor Converter Fed BLDC Motor Drive	342
7.5	Control of Isolated PFC Converters Fed BLDC Motor Drives	344
7.6	MATLAB Based Modeling and Simulation of Isolated PFC Converters Fed BLDC Motor Drives	345
7.7	Hardware Implementation of Isolated PFC Converters Fed BLDC Motor Drives	346
7.8	Results and Discussion	347
7.8.1	Performance of Isolated PFC Flyback Converter Fed BLDC Motor Drive	347
7.8.1.1	Steady State Performance	347
7.8.1.2	Dynamic Performance During Starting and Speed Control	348
7.8.1.3	Dynamic Performance Under Load Variation and Supply Voltage Fluctuation	349
7.8.1.4	Power Quality Performance at Variable Speeds and Different Supply Voltages	350
7.8.2	Performance of Isolated PFC Cuk Converter Fed BLDC Motor Drive	351
7.8.2.1	Steady State Performance	352
7.8.2.2	Dynamic Performance During Starting and Speed Control	354
7.8.2.3	Dynamic Performance Under Load Variation and Supply Voltage Fluctuation	356
7.8.2.4	Power Quality Performance at Variable Speeds and Different Supply Voltages	358
7.8.3	Performance of Isolated PFC SEPIC Fed BLDC Motor Drive	361
7.8.3.1	Steady State Performance	361
7.8.3.2	Dynamic Performance During Starting and Speed Control	362
7.8.3.3	Dynamic Performance Under Load Variation and Supply Voltage Fluctuation	363

7.8.3.4	Power Quality Performance at Variable Speeds and Different Supply Voltages	363
7.8.4	Performance of Isolated PFC Zeta Converter Fed BLDC Motor Drive	365
7.8.4.1	Steady State Performance	365
7.8.4.2	Dynamic Performance During Starting and Speed Control	367
7.8.4.3	Dynamic Performance Under Load Variation and Supply Voltage Fluctuation	369
7.8.4.4	Power Quality Performance at Variable Speeds and Different Supply Voltages	370
7.8.5	Performance of Isolated PFC Luo Converter Fed BLDC Motor Drive	373
7.8.5.1	Steady State Performance	373
7.8.5.2	Dynamic Performance During Starting and Speed Control	374
7.8.5.3	Dynamic Performance Under Load Variation and Supply Voltage Fluctuation	375
7.8.5.4	Power Quality Performance at Variable Speeds and Different Supply Voltages	375
7.8.6	Performance of Isolated PFC Sheppard-Taylor Converter Fed BLDC Motor Drive	377
7.8.6.1	Steady State Performance	377
7.8.6.2	Dynamic Performance During Starting and Speed Control	378
7.8.6.3	Dynamic Performance Under Load Variation and Supply Voltage Fluctuation	378
7.8.6.4	Power Quality Performance at Variable Speeds and Different Supply Voltages	379
7.9	Comparative Evaluation of Various Isolated PFC Converters Fed BLDC Motor Drives	381
7.9.1	Comparison on the Basis of Number of Components of PFC Converter	381
7.9.2	Comparison on the Basis of Improved Power Quality Operation	381
7.9.3	Comparison on the Basis of Stress on PFC Converter Switches	382
7.9.4	Comparison on the Basis of Application Potential and EMI Issues	383
7.10	Conclusions	384
CHAPTER VIII	DESIGN, MODELING AND IMPLEMENTATION OF BRIDGELESS ISOLATED PFC CONVERTERS FED BLDC MOTOR DRIVES	386-463
8.1	General	386

8.2	Classification of Bridgeless Isolated PFC Converters Fed BLDC Motor Drive	387
8.3	Configurations and Operating Principle of Bridgeless Isolated PFC Converters Fed BLDC Motor Drives	388
8.3.1	Bridgeless Isolated PFC Flyback Converter Fed BLDC Motor Drive	388
8.3.2	Bridgeless Isolated PFC Cuk Converter Fed BLDC Motor Drive	391
8.3.3	Bridgeless Isolated PFC SEPIC Fed BLDC Motor Drive	394
8.3.4	Bridgeless Isolated PFC Zeta Converter Fed BLDC Motor Drive	397
8.3.5	Bridgeless Isolated PFC Luo Converter Fed BLDC Motor Drive	400
8.3.6	Bridgeless Isolated PFC Sheppard-Taylor Converter Fed BLDC Motor Drive	403
8.4	Design of Bridgeless Non-Isolated PFC Converters Fed BLDC Motor Drives	408
8.4.1	Bridgeless Isolated PFC Flyback Converter Fed BLDC Motor Drive	411
8.4.2	Bridgeless Isolated PFC Cuk Converter Fed BLDC Motor Drive	412
8.4.3	Bridgeless Isolated PFC SEPIC Fed BLDC Motor Drive	416
8.4.4	Bridgeless Isolated PFC Zeta Converter Fed BLDC Motor Drive	418
8.4.5	Bridgeless Isolated PFC Luo Converter Fed BLDC Motor Drive	420
8.4.6	Bridgeless Isolated PFC Sheppard-Taylor Converter Fed BLDC Motor Drive	422
8.5	Control of Bridgeless Isolated PFC Converters Fed BLDC Motor Drives	425
8.6	MATLAB Based Modeling and Simulation of Bridgeless Isolated PFC Converters Fed BLDC Motor Drives	426
8.7	Hardware Implementation of Bridgeless Isolated PFC Converters Fed BLDC Motor Drives	428
8.8	Results and Discussion	428
8.8.1	Performance of Bridgeless Isolated PFC Flyback Converter Fed BLDC Motor Drive	428
8.8.1.1	Steady State Performance	428
8.8.1.2	Dynamic Performance During Starting and Speed Control	430
8.8.1.3	Dynamic Performance Under Load Variation and Supply Voltage Fluctuation	431
8.8.1.4	Power Quality Performance at Variable Speeds and Different Supply Voltages	431
8.8.2	Performance of Bridgeless Isolated PFC Cuk Converter Fed BLDC Motor Drive	433
8.8.2.1	Steady State Performance	433
8.8.2.2	Dynamic Performance During Starting and Speed Control	436

8.8.2.3	Dynamic Performance Under Load Variation and Supply Voltage Fluctuation	438
8.8.2.4	Power Quality Performance at Variable Speeds and Different Supply Voltages	439
8.8.3	Performance of Bridgeless Isolated PFC SEPIC Fed BLDC Motor Drive	442
8.8.3.1	Steady State Performance	442
8.8.3.2	Dynamic Performance During Starting and Speed Control	443
8.8.3.3	Dynamic Performance Under Load Variation and Supply Voltage Fluctuation	444
8.8.3.4	Power Quality Performance at Variable Speeds and Different Supply Voltages	444
8.8.4	Performance of Bridgeless Isolated PFC Zeta Converter Fed BLDC Motor Drive	446
8.8.4.1	Steady State Performance	446
8.8.4.2	Dynamic Performance During Starting and Speed Control	447
8.8.4.3	Dynamic Performance Under Load Variation and Supply Voltage Fluctuation	448
8.8.4.4	Power Quality Performance at Variable Speeds and Different Supply Voltages	448
8.8.5	Performance of Bridgeless Isolated PFC Luo Converter Fed BLDC Motor Drive	450
8.8.5.1	Steady State Performance	450
8.8.5.2	Dynamic Performance During Starting and Speed Control	451
8.8.5.3	Dynamic Performance Under Load Variation and Supply Voltage Fluctuation	452
8.8.5.4	Power Quality Performance at Variable Speeds and Different Supply Voltages	452
8.8.6	Performance of Bridgeless Isolated PFC Sheppard-Taylor Converter Fed BLDC Motor Drive	454
8.8.6.1	Steady State Performance	454
8.8.6.2	Dynamic Performance During Starting and Speed Control	455
8.8.6.3	Dynamic Performance Under Load Variation and Supply Voltage Fluctuation	456
8.8.6.4	Power Quality Performance at Variable Speeds and Different Supply Voltages	456
8.9	Comparative Evaluation of Various Isolated Bridgeless PFC Converters Fed BLDC Motor Drives	458
8.9.1	Comparison on the Basis of Number of Components of PFC Converter	458

8.9.2	Comparison on the Basis of Improved Power Quality Operation	459
8.9.3	Comparison on the Basis of Stress on PFC Converter Switches	460
8.9.4	Comparison on the Basis of Application Potential and EMI Issues	461
8.10	Conclusions	462

CHAPTER IX DESIGN, MODELING AND IMPLEMENTATION OF INTEGRATED AND HIGH QUALITY RECTIFIERS FED BLDC MOTOR DRIVES 464-542

9.1	General	464
9.2	Classification of Integrated and High Quality Rectifiers Fed BLDC Motor Drives	464
9.3	Configurations and Operating Principle of Integrated and High Quality Rectifiers Fed BLDC Motor Drives	465
9.3.1	Non-Isolated PFC BIFRED Converter Fed BLDC Motor Drive	465
9.3.2	Non-Isolated PFC BIBRED Converter Fed BLDC Motor Drive	468
9.3.3	Non-Isolated PFC Integrated Buck-Boost Buck Converter Fed BLDC Motor Drive	470
9.3.4	Isolated PFC BIFRED Converter Fed BLDC Motor Drive	473
9.3.5	Isolated PFC BIBRED Converter Fed BLDC Motor Drive	475
9.3.6	Isolated PFC Boost-Flyback SSIPP Fed BLDC Motor Drive	478
9.3.7	Isolated PFC Boost-Forward SSIPP Fed BLDC Motor Drive	480
9.4	Design of Integrated and High Quality Rectifiers Fed BLDC Motor Drives	482
9.4.1	Non-Isolated PFC BIFRED Converter Fed BLDC Motor Drive	486
9.4.2	Non-Isolated PFC BIBRED Converter Fed BLDC Motor Drive	489
9.4.3	Non-Isolated PFC Integrated Buck-Boost Buck Converter Fed BLDC Motor Drive	490
9.4.4	Isolated PFC BIFRED Converter Fed BLDC Motor Drive	492
9.4.5	Isolated PFC BIBRED Converter Fed BLDC Motor Drive	495
9.4.6	Isolated PFC Boost-Flyback SSIPP Fed BLDC Motor Drive	497
9.4.7	Isolated PFC Boost-Forward SSIPP Fed BLDC Motor Drive	499
9.5	Control of Integrated and High Quality Rectifiers Fed BLDC Motor Drive	503
9.6	MATLAB Based Modeling and Simulation of Integrated and High Quality Rectifiers Fed BLDC Motor Drive	504

9.7	Hardware Implementation of Integrated and High Quality Rectifiers Fed BLDC Motor Drive	504
9.8	Results and Discussion	505
9.8.1	Performance of Non-Isolated PFC BIFRED Converter Fed BLDC Motor Drive	506
9.8.1.1	Steady State Performance	506
9.8.1.2	Dynamic Performance During Starting and Speed Control	508
9.8.1.3	Dynamic Performance Under Load Variation and Supply Voltage Fluctuation	510
9.8.1.4	Power Quality Performance at Variable Speeds and Different Supply Voltages	511
9.8.2	Performance of Non-Isolated PFC BIBRED Converter Fed BLDC Motor Drive	514
9.8.2.1	Steady State Performance	514
9.8.2.2	Dynamic Performance During Starting and Speed Control	515
9.8.2.3	Dynamic Performance Under Load Variation and Supply Voltage Fluctuation	516
9.8.2.4	Power Quality Performance at Variable Speeds and Different Supply Voltages	516
9.8.3	Performance of Non-Isolated PFC Integrated Buck-Boost Buck Converter Fed BLDC Motor Drive	518
9.8.3.1	Steady State Performance	518
9.8.3.2	Dynamic Performance During Starting and Speed Control	519
9.8.3.3	Dynamic Performance Under Load Variation and Supply Voltage Fluctuation	520
9.8.3.4	Power Quality Performance at Variable Speeds and Different Supply Voltages	520
9.8.4	Performance of Isolated PFC BIFRED Converter Fed BLDC Motor Drive	522
9.8.4.1	Steady State Performance	522
9.8.4.2	Dynamic Performance During Starting and Speed Control	523
9.8.4.3	Dynamic Performance Under Load Variation and Supply Voltage Fluctuation	524
9.8.4.4	Power Quality Performance at Variable Speeds and Different Supply Voltages	524

9.8.5	Performance of Isolated PFC BIBRED Converter Fed BLDC Motor Drive	526
9.8.5.1	Steady State Performance	526
9.8.5.2	Dynamic Performance During Starting and Speed Control	527
9.8.5.3	Dynamic Performance Under Load Variation and Supply Voltage Fluctuation	528
9.8.5.4	Power Quality Performance at Variable Speeds and Different Supply Voltages	528
9.8.6	Performance of Isolated PFC Boost-Flyback SSIPP Fed BLDC Motor Drive	530
9.8.6.1	Steady State Performance	530
9.8.6.2	Dynamic Performance During Starting and Speed Control	531
9.8.6.3	Dynamic Performance Under Load Variation and Supply Voltage Fluctuation	531
9.8.6.4	Power Quality Performance at Variable Speeds and Different Supply Voltages	532
9.8.7	Performance of Isolated PFC Boost-Forward SSIPP Fed BLDC Motor Drive	534
9.8.7.1	Steady State Performance	534
9.8.7.2	Dynamic Performance During Starting and Speed Control	535
9.8.7.3	Dynamic Performance Under Load Variation and Supply Voltage Fluctuation	535
9.8.7.4	Power Quality Performance at Variable Speeds and Different Supply Voltages	536
9.9	Comparative Evaluation of Various Integrated and High Quality Rectifiers Fed BLDC Motor Drives	538
9.9.1	Comparison on the Basis of Number of Components of PFC Converter	538
9.9.2	Comparison on the Basis of Improved Power Quality Operation	538
9.9.3	Comparison on the Basis of Stress on PFC Converter Switches	539
9.9.4	Comparison on the Basis of Application Potential and EMI Issues	540
9.10	Conclusions	542

CHAPTER X DESIGN, MODELING AND IMPLEMENTATION OF SENSORLESS CONTROL OF BLDC MOTOR DRIVE WITH POWER FACTOR CORRECTION 543-602

10.1	General	543
10.2	Configurations of PFC Converters Feeding Sensorless BLDC Motor Drive	544
10.2.1	Non-Isolated PFC Converters Feeding Sensorless BLDC Motor Drive	544
10.2.2	Bridgeless Non-Isolated PFC Converters Feeding Sensorless BLDC Motor Drive	545
10.2.3	Isolated PFC Converters Feeding Sensorless BLDC Motor Drive	545
10.2.4	Bridgeless Isolated PFC Converters Feeding Sensorless BLDC Motor Drive	546
10.2.5	Integrated and High Quality Rectifiers Feeding Sensorless BLDC Motor Drive	547
10.3	Sensorless Control of BLDC Motor Drive Using Rotor Position Phase Delay Compensation	547
10.3.1	Circuit Configuration for Generation of Virtual Hall Signals	547
10.3.2	Design and Selection of Components for Virtual Hall Signals Generation	549
10.3.2.1	Design of a Voltage Sensing Circuitry	549
10.3.2.2	Design of a Hysteresis Comparator	550
10.3.2.3	Design of Isolation Circuitry	553
10.3.3	Measurement of Phase Delay between Actual and Virtual Hall Signals	553
10.3.4	Design of Phase Lead Compensator and Hardware Realization	553
10.3.5	Percentage Error in Phase Delay After Compensation	558
10.4	Control of PFC Converters Feeding Sensorless BLDC Motor Drive	559
10.4.1	Master Control Unit	559
10.4.1.1	Reference Voltage Generation	559
10.4.1.2	BLDC Motor Mode Selection	560
10.4.2	PFC and DC Link Voltage Control Unit	561
10.4.2.1	Voltage Error Generator	561
10.4.2.2	Voltage Controller	561
10.4.2.3	PWM Generator	562
10.4.3	Sensorless Control Unit	562
10.4.3.1	Rotor Position Alignment	562
10.4.3.2	Sensorless Starting Mode-I & II	562
10.4.3.3	Sensorless Operating Mode	564
10.4.3.4	Synchronization	564
10.5	MATLAB Based Modeling and Simulation of PFC Based Sensorless BLDC Motor Drives	565

10.6	Hardware Implementation of PFC Based Sensorless BLDC Motor Drives	565
10.7	Results and Discussion	566
10.7.1	Non-Isolated PFC Converters Feeding Sensorless BLDC Motor Drive	566
10.7.1.1	Steady State Performance	566
10.7.1.2	Dynamic Performance During Starting and Speed Control	568
10.7.1.3	Dynamic Performance Under Load Variation and Supply Voltage Fluctuation	568
10.7.1.4	Power Quality Performance at Variable Speeds and Different Supply Voltages	570
10.7.2	Bridgeless Non-Isolated PFC Converters Feeding Sensorless BLDC Motor Drive	569
10.7.2.1	Steady State Performance	569
10.7.2.2	Dynamic Performance During Starting and Speed Control	570
10.7.2.3	Dynamic Performance Under Load Variation and Supply Voltage Fluctuation	575
10.7.2.4	Power Quality Performance at Variable Speeds and Different Supply Voltages	577
10.7.3	Isolated PFC Converters Feeding Sensorless BLDC Motor Drive	579
10.7.3.1	Steady State Performance	579
10.7.3.2	Dynamic Performance During Starting and Speed Control	581
10.7.3.3	Dynamic Performance Under Load Variation and Supply Voltage Fluctuation	581
10.7.3.4	Power Quality Performance at Variable Speeds and Different Supply Voltages	583
10.7.4	Bridgeless Isolated PFC Converters Feeding Sensorless BLDC Motor Drive	586
10.7.4.1	Steady State Performance	586
10.7.4.2	Dynamic Performance During Starting and Speed Control	587
10.7.4.3	Dynamic Performance Under Load Variation and Supply Voltage Fluctuation	587
10.7.4.4	Power Quality Performance at Variable Speeds and Different Supply Voltages	589
10.7.5	Integrated and High Quality Rectifiers Feeding Sensorless BLDC Motor Drive	592
10.7.5.1	Steady State Performance	592
10.7.5.2	Dynamic Performance During Starting and Speed Control	594

10.7.5.3	Dynamic Performance Under Load Variation and Supply Voltage Fluctuation	595
10.7.5.4	Power Quality Performance at Variable Speeds and Different Supply Voltages	596
10.8	Comparative Performance of Various PFC Converters Feeding Sensorless BLDC Motor Drives	599
10.8.1	Comparison on the Basis of Number of Components of PFC Converter	599
10.8.2	Comparison on the Basis of Application Potential and EMI Issues	601
10.9	Conclusions	601
 CHAPTER XI MAIN CONCLUSIONS AND SUGGESTIONS FOR FURTHER WORK		603-609
11.1	General	603
11.2	Main Conclusions	603
11.3	Suggestions for Further Work	608
 REFERENCES		610-635
 APPENDICES		636-639
 LIST OF PUBLICATIONS		640-343
 BIO-DATA		644-644

LIST OF FIGURES

- Fig. 3.1 Classifications of a PFC converter feeding BLDC motor drives.
- Fig. 3.2 A BLDC motor drive fed by non-isolated PFC based (a) buck-boost converter and (a-b) (b) Cuk converter.
- Fig. 3.3 A BLDC motor drive fed by non-isolated PFC based (a) SEPIC and (b) Zeta (a-b) converter.
- Fig. 3.4 A BLDC motor drive fed by non-isolated PFC based (a) Luo converter and (b) (a-b) CSC converter.
- Fig. 3.5 A BLDC motor drive fed by non-isolated PFC based (a) Sheppard-Taylor (a-b) converter and (b) SC-buck-Boost converter.
- Fig. 3.6 A BLDC motor drive fed by bridgeless non-isolated PFC based (a) buck-boost (a-b) converter and (b) Cuk converter.
- Fig. 3.7 A BLDC motor drive fed by bridgeless non-isolated PFC based (a) SEPIC and (b) (a-b) Zeta converter.
- Fig. 3.8 A BLDC motor drive fed by bridgeless non-isolated PFC based (a) Luo converter (a-b) and (b) CSC converter.
- Fig. 3.9 A BLDC motor drive fed by bridgeless non-isolated PFC based (a) Sheppard- (a-b) Taylor converter and (b) SC-Buck-Boost converter.
- Fig. 3.10 A BLDC motor drive fed by an isolated PFC based (a) flyback converter and (b) (a-b) Cuk converter.
- Fig. 3.11 A BLDC motor drive fed by an isolated PFC based (a) SEPIC and (b) Zeta (a-b) converter.
- Fig. 3.12 A BLDC motor drive fed by an isolated PFC based (a) Luo and (b) Sheppard- (a-b) Taylor converter.
- Fig. 3.13 A BLDC motor drive fed by a bridgeless isolated PFC based (a) flyback converter (a-b) and (b) Cuk converter.
- Fig. 3.14 A BLDC motor drive fed by a bridgeless isolated PFC based (a) SEPIC and (b) (a-b) Zeta converter.
- Fig. 3.15 A BLDC motor drive fed by a bridgeless isolated PFC based (a) Luo converter and (a-b) (b) Sheppard-Taylor converter.
- Fig. 3.16 A BLDC motor drive fed by a non-isolated PFC based (a) BIFRED and (b) (a-b) BIBRED converter.

- Fig. 3.17 A BLDC motor drive fed by a non-isolated PFC based integrated buck-boost buck converter.
- Fig. 3.18 A BLDC motor drive fed by an isolated PFC based (a) BIFRED and (b) BIBRED converter.
- Fig. 3.19 A BLDC motor drive fed by an isolated PFC based (a) boost-flyback SSIPP and (b) boost-forward SSIPP.
- Fig. 4.1 A diode bridge rectifier (DBR) feeding BLDC motor drive.
- Fig. 4.2 A PFC boost converter fed BLDC motor drive with boost converter operating in CCM.
- Fig. 4.3 A PFC boost converter fed BLDC motor drive with boost converter operating in DCM.
- Fig. 4.4 A PFC buck-boost converter fed BLDC motor drive with boost converter operating in CCM.
- Fig. 4.5 A PFC buck-boost converter fed BLDC motor drive with boost converter operating in DCM.
- Fig. 4.6 Waveforms showing the back-emf and phase current in a BLDC motor operating in PWM mode.
- Fig. 4.7 Waveforms showing the back-emf and phase current in a BLDC motor operating in FFS mode.
- Fig. 4.8 Control unit of a PWM based VSI fed BLDC motor.
- Fig. 4.9 Control unit of a PFC converter operating in CCM with constant DC link voltage.
- Fig. 4.10 Control unit of a PFC converter operating in DCM with constant DC link voltage.
- Fig. 4.11 Control unit of a PFC converter operating in CCM with variable DC link voltage.
- Fig. 4.12 Control unit of a PFC converter operating in DCM with variable DC link voltage.
- Fig. 4.13 Equivalent circuit of a three-phase VSI feeding BLDC motor.
- Fig. 4.14 MATLAB/Simulink model of a BLDC motor drive.
- Fig. 4.15 Hardware prototype of a BLDC motor drive.
- Fig. 4.16 Opto-isolation circuitry (a) schematic diagram and (b) developed hardware prototype.
- Fig. 4.17 Voltage sensing circuitry (a) schematic diagram and (b) developed hardware prototype.
- Fig. 4.18 Current sensing circuitry (a) schematic diagram and (b) developed hardware prototype.

- Fig. 4.19 A TI-TMS320F2813 board used for the development of hardware prototype.
- Fig. 4.20 Simulated steady state performance of a PFC boost converter fed BLDC motor at rated condition with speed maintained at (a) 2500 rpm and (b) 500 rpm.
- Fig. 4.21 Recorded steady state performance of a PFC boost converter fed BLDC motor at rated condition with speed maintained at (a) 2500 rpm and (b) 500 rpm.
- Fig. 4.22 Simulated dynamic performance of DBR fed BLDC motor drive during (a) starting at speed of 500 rpm and (b) step change in speed from 1000 rpm to 2000 rpm at rated conditions.
- Fig. 4.23 Recorded dynamic performance of DBR fed BLDC motor drive during (a) starting at speed of 500 rpm and (b) step change in speed from 1000 rpm to 2000 rpm at rated conditions.
- Fig. 4.24 (a) Simulated and (b) recorded dynamic performance of DBR fed BLDC motor drive during step change in load from 0.4 Nm to 0.8 Nm at rated conditions.
- Fig. 4.25 Simulated harmonic spectrum of supply current at AC mains for a conventional DBR fed BLDC motor drive operating at (a) rated speed of 2500 rpm and (b) light speed of 500 rpm.
- Fig. 4.26 Recorded power indices of DBR fed BLDC motor drive at rated load with BLDC motor operating at (a-c) rated speed of 2500 rpm and (d-f) light speed of 500 rpm.
- Fig. 4.27 Simulated steady state performance of a PFC boost converter fed BLDC motor at rated condition with speed maintained at (a) 2500 rpm and (b) 500 rpm.
- Fig. 4.28 Recorded steady state performance of a PFC boost converter fed BLDC motor at rated condition with speed maintained at (a) 2500 rpm and (b) 500 rpm.
- Fig. 4.29 Simulated dynamic performance of PFC boost converter fed BLDC motor drive during (a) starting at speed of 500 rpm and (b) step change in speed from 1000 rpm to 2000 rpm at rated conditions.
- Fig. 4.30 Recorded dynamic performance of PFC boost converter fed BLDC motor drive during (a) starting at speed of 500 rpm and (b) step change in speed from 1000 rpm to 2000 rpm at rated conditions.
- Fig. 4.31 Simulated dynamic performance of a PFC boost converter fed BLDC motor drive during (a) step change in load from 0.4 Nm to 0.8 Nm and (c) step change in supply voltage from 270 V to 170 V.
- Fig. 4.32 Recorded dynamic performance of a PFC boost converter fed BLDC motor drive during (a) step change in load and (b) step change in supply voltage from 270 V to 200 V.

- Fig. 4.33 (a-b) Simulated harmonic spectrum of supply current at AC mains for a PFC boost converter fed BLDC motor drive operating at (a) rated speed of 2500 rpm and (b) light speed of 500 rpm.
- Fig. 4.34 (a-f) Recorded power indices of PFC converter fed BLDC motor drive with constant DC link voltage of VSI at rated load with BLDC motor operating at (a-c) rated speed of 2500 rpm and (d-f) light speed of 500 rpm.
- Fig. 4.35 (a-b) Simulated harmonic spectrum of supply current at AC mains for a PFC boost converter fed BLDC motor drive operating at rated condition with supply voltage as (a) 170 V and (b) 270 V.
- Fig. 4.36 (a-b) Recorded power indices of PFC converter fed BLDC motor drive with constant DC link voltage of VSI at rated condition with BLDC motor operating at supply voltage of (a-c) 170 V and (b) 270 V.
- Fig. 4.37 (a-b) Simulated steady state performance of a PFC buck-boost converter fed BLDC motor at rated loading condition with DC link voltage as (a) 200 V and (b) 50 V.
- Fig. 4.38 (a-b) Recorded steady state performance of a PFC buck-boost converter fed BLDC motor at rated loading condition with DC link voltage as (a) 200 V and (b) 50 V.
- Fig. 4.39 (a-b) Simulated dynamic performance of PFC buck-boost PFC converter fed BLDC motor drive during (a) starting at DC link voltage of 50 V and (b) speed control at change in DC link voltage from 100 V to 150 V.
- Fig. 4.40 (a-b) Recorded dynamic performance of PFC buck-boost PFC converter fed BLDC motor drive during (a) starting at DC link voltage of 50 V and (b) speed control at change in DC link voltage from 100 V to 150 V.
- Fig. 4.41 (a-b) Simulated dynamic performance of a PFC buck-boost converter fed BLDC motor drive during (a) step change in load from 0.4 Nm to 0.8 Nm and (b) step change in supply voltage from 270 V to 170 V.
- Fig. 4.42 (a-b) Recorded dynamic performance of a PFC buck-boost converter fed BLDC motor drive during (a) step change in load and (b) step change in supply voltage from 270 V to 200 V.
- Fig. 4.43 (a-b) Simulated harmonic spectrum of supply current at AC mains for a PFC buck-boost converter fed BLDC motor drive operating at rated condition with DC link voltage as (a) 200 V and (b) 50 V.
- Fig. 4.44 (a-f) Recorded power indices at AC mains for a PFC buck-boost converter fed BLDC motor drive operating at rated condition with DC link voltage as (a-c) 200 V and (d-f) 50 V.
- Fig. 4.45 (a-b) Simulated harmonic spectrum of supply current at AC mains for a PFC buck-boost converter fed BLDC motor drive operating at rated condition with supply voltage as (a) 90 V and (b) 270 V.

- Fig. 4.46 (a-f) Recorded power quality indices at AC mains for a PFC buck-boost converter fed BLDC motor drive operating at rated condition with supply voltage as (a-c) 96 V and (d-f) 271 V.
- Fig. 4.47 (a-b) Comparative evaluation of the three configurations of BLDC motor drives showing (a) the THD of supply current and (b) the power factor at AC mains.
- Fig. 4.48 Comparative evaluation of efficiency of three configurations of BLDC motor drives.
- Fig. 5.1 Circuit configuration of a non-isolated PFC buck-boost converter fed BLDC motor drive.
- Fig. 5.2 (a-c) Different operating modes of a PFC buck-boost converter in DCM and (d) the associated waveforms.
- Fig. 5.3 Circuit configuration of a non-isolated PFC Cuk converter fed BLDC motor drive.
- Fig. 5.4 (a-c) Different operating modes of a PFC Cuk converter in DCM and (d) the associated waveforms.
- Fig. 5.5 Circuit configuration of a non-isolated PFC SEPIC fed BLDC motor drive.
- Fig. 5.6 (a-c) Different operating modes of a PFC SEPIC in DCM and (d) the associated waveforms.
- Fig. 5.7 Circuit configuration of a non-isolated PFC zeta converter fed BLDC motor drive.
- Fig. 5.8 (a-c) Different operating modes of a PFC Zeta converter in DCM and (d) the associated waveforms.
- Fig. 5.9 Circuit configuration of a non-isolated PFC Luo converter fed BLDC motor drive.
- Fig. 5.10 (a-c) Different operating modes of a PFC Luo converter in DCM and (d) the associated waveforms.
- Fig. 5.11 Circuit configuration of a non-isolated PFC CSC converter fed BLDC motor drive.
- Fig. 5.12 (a-c) Different operating modes of a PFC CSC converter in DCM and (d) the associated waveforms.
- Fig. 5.13 Circuit configuration of a non-isolated PFC Sheppard-Taylor converter fed BLDC motor drive.
- Fig. 5.14 (a-d) Different operating modes of a PFC Sheppard-Taylor converter operating in DCM and (e) the associated waveforms.
- Fig. 5.15 Circuit configuration of a PFC switched-capacitor buck-boost converter fed BLDC motor drive.
- Fig. 5.16 (a-c) Different operating modes of a PFC Switched-Capacitor Buck-Boost converter operating in DCM and (d) the associated waveforms.

- Fig. 5.17 Control unit of a PFC converter operating in DCM with variable DC link voltage.
- Fig. 5.18 MATLAB/Simulink model of a non-isolated PFC converter fed BLDC motor drive.
- Fig. 5.19 Simulated steady state performance of a PFC buck-boost converter fed BLDC motor at rated loading condition with DC link voltage as 200 V.
- Fig. 5.20 Recorded steady state performance of a PFC buck-boost converter fed BLDC motor at rated loading condition with DC link voltage as (a) 200 V and (b) 50 V.
- Fig. 5.21 Recorded performance of PFC buck-boost converter fed BLDC motor at rated condition showing (a) inductor current with supply voltage and supply current and (b) voltage and current stress on PFC converter switch.
- Fig. 5.22 Simulated dynamic performance of PFC buck-boost PFC converter fed BLDC motor drive during (a) starting at DC link voltage of 50 V and (b) speed control at change in DC link voltage from 100 V to 150 V.
- Fig. 5.23 Recorded dynamic performance of PFC buck-boost PFC converter fed BLDC motor drive during (a) starting at DC link voltage of 50 V and (b) speed control at change in DC link voltage from 100 V to 150 V.
- Fig. 5.24 Simulated dynamic performance of a PFC buck-boost converter fed BLDC motor drive during (a) step change in load from 0.4 Nm to 0.8 Nm and (c) step change in supply voltage from 270 V to 170 V.
- Fig. 5.25 Recorded dynamic performance of a PFC buck-boost converter fed BLDC motor drive during (a) step change in load and (c) step change in supply voltage from 270 V to 200 V.
- Fig. 5.26 Simulated harmonic spectrum of supply current at AC mains for a PFC buck-boost converter fed BLDC motor drive operating at rated condition with DC link voltage as (a) 200 V and (b) 50 V.
- Fig. 5.27 Recorded power indices at AC mains for a PFC buck-boost converter fed BLDC motor drive operating at rated condition with DC link voltage as (a-c) 200 V and (d-f) 50 V.
- Fig. 5.28 Simulated harmonic spectrum of supply current at AC mains for a PFC buck-boost converter fed BLDC motor drive operating at rated condition with supply voltage as (a) 90 V and (b) 270 V.
- Fig. 5.29 Recorded power quality indices at AC mains for a PFC buck-boost converter fed BLDC motor drive operating at rated condition with supply voltage as (a-c) 96 V and (d-f) 271 V.
- Fig. 5.30 Simulated steady state performance of a PFC Cuk converter fed BLDC motor at rated loading condition with DC link voltage as 200 V.

- Fig. 5.31 (a-b) Recorded steady state performance of a PFC Cuk converter fed BLDC motor at rated loading condition with DC link voltage as (a) 200 V and (b) 50 V.
- Fig. 5.32 (a-b) Recorded performance of PFC Cuk converter fed BLDC motor at rated condition showing (a) i_{Li} , v_{CI} and i_{Lo} with v_s and (b) its enlarged waveforms.
- Fig. 5.33 (a-b) Recorded performance of PFC Cuk converter fed BLDC motor at rated condition showing (a) voltage and current stress on PFC converter switch and (b) its enlarged waveforms.
- Fig. 5.34 (a-b) Simulated dynamic performance of PFC Cuk PFC converter fed BLDC motor drive during (a) starting at DC link voltage of 50 V and (b) speed control at change in DC link voltage from 100 V to 150 V.
- Fig. 5.35 (a-b) Recorded dynamic performance of PFC Cuk PFC converter fed BLDC motor drive during (a) starting at DC link voltage of 50 V and (b) speed control at change in DC link voltage from 100 V to 150 V.
- Fig. 5.36 (a-b) Simulated dynamic performance of a PFC Cuk converter fed BLDC motor drive during (a) step change in load from 0.4 Nm to 0.8 Nm and (b) step change in supply voltage from 270 V to 170 V.
- Fig. 5.37 (a-b) Recorded dynamic performance of a PFC Cuk converter fed BLDC motor drive during (a) step change in load and (b) step change in supply voltage from 270 V to 200 V.
- Fig. 5.38 (a-b) Simulated harmonic spectrum of supply current at AC mains for a PFC Cuk converter fed BLDC motor drive operating at rated condition with DC link voltage as (a) 200 V and (b) 50 V.
- Fig. 5.39 (a-f) Recorded power indices at AC mains for a PFC Cuk converter fed BLDC motor drive operating at rated loading condition with DC link voltage as (a-c) 200 V and (d-f) 50 V.
- Fig. 5.40 (a-b) Simulated harmonic spectrum of supply current at AC mains for a PFC Cuk converter fed BLDC motor drive operating at rated condition with supply voltage as (a) 90 V and (b) 270 V.
- Fig. 5.41 (a-f) Recorded power quality indices at AC mains for a PFC Cuk converter fed BLDC motor drive operating at rated condition with supply voltage as (a-c) 170 V and (d-f) 270 V.
- Fig. 5.42 Simulated steady state performance of a PFC SEPIC fed BLDC motor at rated load condition with DC link voltage as 200 V.
- Fig. 5.43 (a-b) Recorded steady state performance of a PFC SEPIC fed BLDC motor at rated loading condition with DC link voltage as (a) 200 V and (b) 50 V.

- Fig. 5.44 (a-b) Recorded performance of PFC SEPIC fed BLDC motor drive at rated condition showing (a) input inductor current (i_{Li}) and (b) output inductor current (i_{Lo}) with v_s , i_s and V_{dc} .
- Fig. 5.45 (a-b) Recorded performance of PFC Cuk converter fed BLDC motor drive showing (a) intermediate capacitor voltage (v_{CI}) with v_s , i_s and V_{dc} (b) voltage (v_{sw}) and current (i_{sw}) stress on PFC converter switch.
- Fig. 5.46 (a-b) Simulated dynamic performance of PFC SEPIC fed BLDC motor drive during (a) starting at DC link voltage of 50 V and (b) speed control at change in DC link voltage from 100 V to 150 V.
- Fig. 5.47 (a-b) Recorded dynamic performance of PFC SEPIC fed BLDC motor drive during (a) starting at DC link voltage of 50 V and (b) speed control at change in DC link voltage from 100 V to 150 V.
- Fig. 5.48 (a-b) Simulated dynamic performance of a PFC SEPIC fed BLDC motor drive during (a) step change in load from 0.4 Nm to 0.8 Nm and (b) step change in supply voltage from 270 V to 170 V.
- Fig. 5.49 (a-b) Recorded dynamic performance of a PFC SEPIC fed BLDC motor drive during (a) step change in load and (b) step change in supply voltage from 270 V to 200 V.
- Fig. 5.50 (a-b) Simulated harmonic spectrum of supply current at AC mains for a PFC SEPIC fed BLDC motor drive operating at rated condition with DC link voltage as (a) 200 V and (b) 50 V.
- Fig. 5.51 (a-f) Recorded power indices at AC mains for a PFC SEPIC fed BLDC motor drive operating at rated condition with DC link voltage as (a-c) 200 V and (d-f) 50 V.
- Fig. 5.52 (a-b) Simulated harmonic spectrum of supply current at AC mains for a PFC SEPIC fed BLDC motor drive operating at rated condition with supply voltage as (a) 90 V and (b) 270 V.
- Fig. 5.53 (a-f) Recorded power quality indices at AC mains for a PFC SEPIC fed BLDC motor drive operating at rated loading condition with supply voltage as (a-c) 90 V and (d-f) 270 V.
- Fig. 5.54 Simulated steady state performance of a PFC Zeta converter fed BLDC motor drive at rated loading condition with DC link voltage as 200 V.
- Fig. 5.55 (a-b) Recorded steady state performance of a PFC Zeta converter fed BLDC motor drive at rated loading condition with DC link voltage as (a) 200 V and (b) 50 V.
- Fig. 5.56 (a-b) Recorded performance of PFC Zeta converter fed BLDC motor drive at rated condition showing (a) input inductor current (i_{Li}) and (b) output inductor current (i_{Lo}) with v_s , i_s and V_{dc} .

- Fig. 5.57 (a-b) Recorded performance of PFC Zeta converter fed BLDC motor drive showing (a) intermediate capacitor voltage (v_{CI}) with v_s , i_s and V_{dc} (b) voltage (v_{sw}) and current (i_{sw}) stress on PFC converter switch.
- Fig. 5.58 (a-b) Simulated dynamic performance of PFC Zeta converter fed BLDC motor drive during (a) starting at DC link voltage of 50 V and (b) speed control at change in DC link voltage from 100 V to 150 V.
- Fig. 5.59 (a-b) Recorded dynamic performance of PFC Zeta converter fed BLDC motor drive during (a) starting at DC link voltage of 50 V and (b) speed control at change in DC link voltage from 100 V to 150 V.
- Fig. 5.60 (a-b) Simulated dynamic performance of a PFC Zeta converter fed BLDC motor drive during (a) step change in load from 0.4 Nm to 0.8 Nm and (b) step change in supply voltage from 270 V to 170 V.
- Fig. 5.61 (a-b) Recorded dynamic performance of a PFC Zeta converter fed BLDC motor drive during (a) step change in load and (b) step change in supply voltage from 270 V to 200 V.
- Fig. 5.62 (a-b) Simulated harmonic spectrum of supply current at AC mains for a PFC Zeta converter fed BLDC motor drive operating at rated condition with DC link voltage as (a) 200 V and (b) 50 V.
- Fig. 5.63 (a-f) Recorded power indices at AC mains for a PFC Zeta converter fed BLDC motor drive operating at rated loading condition with DC link voltage as (a-c) 200 V and (d-f) 50 V.
- Fig. 5.64 (a-b) Simulated harmonic spectrum of supply current at AC mains for a PFC Zeta converter fed BLDC motor drive operating at rated condition with supply voltage as (a) 90 V and (b) 270 V.
- Fig. 5.65 (a-f) Recorded power quality indices at AC mains for a PFC Zeta converter fed BLDC motor drive operating at rated condition with supply voltage as (a-c) 90 V and (d-f) 270 V.
- Fig. 5.66 Simulated steady state performance of a PFC Luo converter fed BLDC motor drive at rated loading condition with DC link voltage as 200 V.
- Fig. 5.67 (a-b) Recorded steady state performance of a PFC Luo converter fed BLDC motor drive at rated loading condition with DC link voltage as (a) 200 V and (b) 50 V.
- Fig. 5.68 (a-b) Recorded performance of PFC Luo converter fed BLDC motor drive at rated condition showing (a) inductor currents (i_{Li} and i_{Lo}) and intermediate capacitor voltage (v_{CI}) with v_s and (b) its enlarged waveforms.
- Fig. 5.69 (a-b) Recorded performance of PFC Luo converter fed BLDC motor drive at rated condition showing (a) voltage (v_{sw}) and current (i_{sw}) stress on PFC converter switch with v_s and (b) its enlarged waveforms.

- Fig. 5.70 (a-b) Simulated dynamic performance of PFC Luo converter fed BLDC motor drive during (a) starting at DC link voltage of 50 V and (b) speed control at change in DC link voltage from 100 V to 150 V.
- Fig. 5.71 (a-b) Recorded dynamic performance of PFC Luo converter fed BLDC motor drive during (a) starting at DC link voltage of 50 V and (b) speed control at change in DC link voltage from 100 V to 150 V.
- Fig. 5.72 (a-b) Simulated dynamic performance of a PFC Luo converter fed BLDC motor drive during (a) step change in load from 0.4 Nm to 0.8 Nm and (b) step change in supply voltage from 270 V to 170 V.
- Fig. 5.73 (a-b) Recorded dynamic performance of a PFC Luo converter fed BLDC motor drive during (a) step change in load and (b) step change in supply voltage from 270 V to 200 V.
- Fig. 5.74 (a-b) Simulated harmonic spectrum of supply current at AC mains for a PFC Luo converter fed BLDC motor drive operating at rated condition with DC link voltage as (a) 200 V and (b) 50 V.
- Fig. 5.75 (a-f) Recorded power indices at AC mains for a PFC Luo converter fed BLDC motor drive operating at rated loading condition with DC link voltage as (a-c) 200 V and (d-f) 50 V.
- Fig. 5.76 (a-b) Simulated harmonic spectrum of supply current at AC mains for a PFC Luo converter fed BLDC motor drive operating at rated condition with supply voltage as (a) 90 V and (b) 270 V.
- Fig. 5.77 (a-f) Recorded power quality indices at AC mains for a PFC Luo converter fed BLDC motor drive operating at rated condition with supply voltage as (a-c) 110 V and (d-f) 260 V.
- Fig. 5.78 Simulated steady state performance of a PFC CSC converter fed BLDC motor at rated loading condition with DC link voltage as 200 V.
- Fig. 5.79 (a-b) Recorded steady state performance of a PFC Luo converter fed BLDC motor at rated loading condition with DC link voltage as (a) 200 V and (b) 50 V.
- Fig. 5.80 (a-b) Recorded performance of PFC CSC converter fed BLDC motor drive at rated condition showing (a) discontinuous inductor current (i_{Li}) and (b) continuous intermediate capacitor voltage (v_{CI}) with v_s , i_s and V_{dc} .
- Fig. 5.81 (a-b) Recorded performance of PFC CSC converter fed BLDC motor drive at rated condition showing (a) voltage (v_{sw}) and current (i_{sw}) stress on PFC converter switch with v_s and i_s and (b) its enlarged waveforms.
- Fig. 5.82 (a-b) Simulated dynamic performance of PFC CSC converter fed BLDC motor drive during (a) starting at DC link voltage of 50 V and (b) speed control at change in DC link voltage from 100 V to 150 V.

- Fig. 5.83 (a-b) Recorded dynamic performance of PFC CSC converter fed BLDC motor drive during (a) starting at DC link voltage of 50 V and (b) speed control at change in DC link voltage from 100 V to 150 V.
- Fig. 5.84 (a-b) Simulated dynamic performance of a PFC CSC converter fed BLDC motor drive during (a) step change in load from 0.4 Nm to 0.8 Nm and (b) step change in supply voltage from 270 V to 170 V.
- Fig. 5.85 (a-b) Recorded dynamic performance of a PFC CSC converter fed BLDC motor drive during (a) step change in load and (b) step change in supply voltage from 270 V to 200 V.
- Fig. 5.86 (a-b) Simulated harmonic spectrum of supply current at AC mains for a PFC CSC converter fed BLDC motor drive operating at rated condition with DC link voltage as (a) 200 V and (b) 50 V.
- Fig. 5.87 (a-f) Recorded power indices at AC mains for a PFC CSC converter fed BLDC motor drive operating at rated loading condition with DC link voltage as (a-c) 200 V and (d-f) 50 V.
- Fig. 5.88 (a-b) Simulated harmonic spectrum of supply current at AC mains for a PFC CSC converter fed BLDC motor drive operating at rated condition with supply voltage as (a) 90 V and (b) 270 V.
- Fig. 5.89 (a-f) Recorded power quality indices at AC mains for a PFC CSC converter fed BLDC motor drive operating at rated condition with supply voltage as (a-c) 90 V and (d-f) 270 V.
- Fig. 5.90 Simulated steady state performance of a PFC Sheppard-Taylor converter fed BLDC motor at rated loading condition with DC link voltage as 200 V.
- Fig. 5.91 (a-b) Simulated dynamic performance of PFC Sheppard-Taylor converter fed BLDC motor drive during (a) starting at DC link voltage of 50 V and (b) speed control at change in DC link voltage from 100 V to 150 V.
- Fig. 5.92 (a-b) Simulated dynamic performance of a PFC Sheppard-Taylor converter fed BLDC motor drive during (a) step change in load from 0.4 Nm to 0.8 Nm and (c) step change in supply voltage from 270 V to 170 V.
- Fig. 5.93 (a-b) Simulated harmonic spectrum of supply current at AC mains for a PFC Sheppard-Taylor converter fed BLDC motor drive operating at rated condition with DC link voltage as (a) 200 V and (b) 50 V.
- Fig. 5.94 (a-b) Simulated harmonic spectrum of supply current at AC mains for a PFC Sheppard-Taylor converter fed BLDC motor drive operating at rated condition with supply voltage as (a) 90 V and (b) 270 V.
- Fig. 5.95 Simulated steady state performance of a PFC switched capacitor buck boost converter fed BLDC motor at rated condition with DC link voltage as 200 V.

- Fig. 5.96 (a-b) Simulated performance of PFC switched capacitor buck boost converter fed BLDC motor drive during (a) starting at DC link voltage of 50 V and (b) speed control at change in DC link voltage from 100 V to 150 V.
- Fig. 5.97 (a-b) Simulated dynamic performance of a PFC switched capacitor buck boost converter fed BLDC motor drive during (a) step change in load from 0.4 Nm to 0.8 Nm and (b) step change in supply voltage from 270 V to 170 V.
- Fig. 5.98 (a-b) Simulated harmonic spectrum of supply current at AC mains for a PFC switched capacitor buck boost converter fed BLDC motor drive operating at rated condition with DC link voltage as (a) 200 V and (b) 50 V.
- Fig. 5.99 (a-b) Simulated harmonic spectrum of supply current at AC mains for a PFC switched capacitor buck boost converter fed BLDC motor drive operating at rated condition with supply voltage as (a) 90 V and (b) 270 V.
- Fig. 6.1 Circuit configuration of a bridgeless non-isolated PFC buck-boost converter fed BLDC motor drive.
- Fig. 6.2 (a-f) Operation of bridgeless PFC buck-boost converter showing different modes of operations as (a) Mode P-I, (b) Mode P-II, (c) Mode P-III, (d) Mode N-I, (e) Mode N-II, (f) Mode N-III respectively.
- Fig. 6.3 (a-b) Operating waveforms of PFC based bridgeless non-isolated buck-boost converter in (a) line cycle and (b) complete switching cycle.
- Fig. 6.4 Circuit configuration of a bridgeless non-isolated PFC Cuk converter fed BLDC motor drive.
- Fig. 6.5 (a-f) Operation of bridgeless non-isolated PFC Cuk converter showing different modes of operations as (a) Mode P-I, (b) Mode P-II, (c) Mode P-III, (d) Mode N-I, (e) Mode N-II, (f) Mode N-III respectively.
- Fig. 6.6 (a-b) Operating waveforms of PFC based bridgeless non-isolated Cuk in (a) line cycle and (b) complete switching cycle.
- Fig. 6.7 Circuit configuration of a bridgeless non-isolated PFC SEPIC fed BLDC motor drive.
- Fig. 6.8 (a-f) Operation of bridgeless non-isolated PFC SEPIC showing different modes of operations as (a) Mode P-I, (b) Mode P-II, (c) Mode P-III, (d) Mode N-I, (e) Mode N-II, (f) Mode N-III respectively.
- Fig. 6.9 (a-b) Operating waveforms of PFC based bridgeless non-isolated SEPIC in (a) line cycle and (b) complete switching cycle.
- Fig. 6.10 Circuit configuration of a bridgeless non-isolated PFC Zeta converter fed BLDC motor drive.

- Fig. 6.11 (a-f) Operation of bridgeless non-isolated PFC Zeta converter showing different modes of operations as (a) Mode P-I, (b) Mode P-II, (c) Mode P-III, (d) Mode N-I, (e) Mode N-II, (f) Mode N-III respectively.
- Fig. 6.12 (a-b) Operating waveforms of PFC based bridgeless non-isolated Zeta converter in (a) line cycle and (b) complete switching cycle.
- Fig. 6.13 Circuit configuration of a bridgeless non-isolated PFC Luo converter fed BLDC motor drive.
- Fig. 6.14 (a-f) Operation of bridgeless non-isolated PFC Luo converter showing different modes of operations as (a) Mode P-I, (b) Mode P-II, (c) Mode P-III, (d) Mode N-I, (e) Mode N-II, (f) Mode N-III respectively.
- Fig. 6.15 (a-b) Operating waveforms of PFC based bridgeless non-isolated Luo converter in (a) line cycle and (b) complete switching cycle.
- Fig. 6.16 Circuit configuration of a bridgeless non-isolated PFC CSC converter fed BLDC motor drive.
- Fig. 6.17 (a-f) Operation of bridgeless non-isolated PFC CSC converter showing different modes of operations as (a) Mode P-I, (b) Mode P-II, (c) Mode P-III, (d) Mode N-I, (e) Mode N-II, (f) Mode N-III respectively.
- Fig. 6.18 (a-b) Operating waveforms of PFC based bridgeless non-isolated CSC converter in (a) line cycle and (b) complete switching cycle.
- Fig. 6.19 Circuit configuration of a bridgeless non-isolated PFC Sheppard-Taylor converter fed BLDC motor drive.
- Fig. 6.20 (a-d) Different modes of operation of bridgeless non-isolated PFC Sheppard-Taylor for positive half cycle of supply voltage as (a) Mode P-I, (b) Mode P-II, (c) Mode P-III and (d) Mode P-IV respectively.
- Fig. 6.21 (a-d) Different modes of operation of bridgeless non-isolated PFC Sheppard-Taylor for negative half cycle of supply voltage as (a) Mode N-I, (b) Mode N-II, (c) Mode N-III and (d) Mode N-IV respectively.
- Fig. 6.22 (a-b) Operating waveforms of bridgeless non-isolated PFC Sheppard-Taylor converter in (a) line cycle and (b) complete switching cycle.
- Fig. 6.23 Circuit configuration of a bridgeless non-isolated PFC SC buck-boost converter fed BLDC motor drive.
- Fig. 6.24 (a-f) Operation of bridgeless non-isolated PFC SC buck-boost converter showing different modes of operations as (a) Mode P-I, (b) Mode P-II, (c) Mode P-III, (d) Mode N-I, (e) Mode N-II, (f) Mode N-III respectively.
- Fig. 6.25 (a-b) Operating waveforms of bridgeless non-isolated PFC switched-capacitor buck-boost converter in (a) line cycle and (b) complete switching cycle.

- Fig. 6.26 Control unit of a PFC converter operating in DCM with variable DC link voltage.
- Fig. 6.27 MATLAB/Simulink model of an Isolated PFC converter fed BLDC motor drive.
- Fig. 6.28 Simulated steady state performance of a bridgeless PFC buck-boost converter fed BLDC motor at rated loading condition with DC link voltage as 200 V.
- Fig. 6.29 Recorded steady state performance of a bridgeless PFC buck-boost converter fed BLDC motor at rated loading condition with DC link voltage as (a) 200 V and (b) 50 V.
- Fig. 6.30 Recorded performance of bridgeless PFC buck-boost converter fed BLDC motor at rated condition showing (a) discontinuous inductor currents (i_{Li1} and i_{Li2}) and (b) its enlarged waveforms.
- Fig. 6.31 Recorded performance of bridgeless PFC buck-boost converter fed BLDC motor at rated condition showing (a) voltage (v_{sw1} , v_{sw2}) and current (i_{sw1} , i_{sw2}) stress on solid-state switches and (b) its enlarged waveforms.
- Fig. 6.32 Simulated dynamic performance of bridgeless PFC buck-boost converter fed BLDC motor drive during (a) starting at DC link voltage of 50 V and (b) speed control at change in DC link voltage from 100 V to 150 V.
- Fig. 6.33 Recorded dynamic performance of bridgeless PFC buck-boost converter fed BLDC motor drive during (a) starting at DC link voltage of 50 V and (b) speed control at change in DC link voltage from 100 V to 150 V.
- Fig. 6.34 Simulated dynamic performance of a bridgeless PFC buck-boost converter fed BLDC motor drive during (a) step change in load from 0.4 Nm to 0.8 Nm and (b) step change in supply voltage from 270 V to 170 V.
- Fig. 6.35 Recorded dynamic performance of a bridgeless PFC buck-boost converter fed BLDC motor drive during (a) step change in load and (b) step change in supply voltage from 270 V to 200 V.
- Fig. 6.36 Simulated harmonic spectrum of supply current at AC mains for a bridgeless PFC buck-boost converter fed BLDC motor drive operating at rated condition with DC link voltage as (a) 200 V and (b) 50 V.
- Fig. 6.37 Recorded power indices at AC mains for a bridgeless PFC buck-boost converter fed BLDC motor drive operating at rated condition with DC link voltage as (a-c) 200 V and (d-f) 50 V.
- Fig. 6.38 Simulated harmonic spectrum of supply current at AC mains for a bridgeless PFC buck-boost converter fed BLDC motor drive operating at rated condition with supply voltage as (a) 90 V and (b) 270 V.
- Fig. 6.39 Recorded power quality indices at AC mains for a bridgeless PFC buck-boost converter fed BLDC motor drive operating at rated condition with supply voltage as (a-c) 90 V and (d-f) 270 V.

- Fig. 6.40 (a-b) Simulated steady state performance of a bridgeless PFC Cuk converter fed BLDC motor at rated loading condition with DC link voltage as 200 V.
- Fig. 6.41 (a-b) Recorded steady state performance of a bridgeless PFC Cuk converter fed BLDC motor at rated loading condition with DC link voltage as (a) 200 V and (b) 50 V.
- Fig. 6.42 (a-b) Recorded performance of bridgeless non-isolated PFC Cuk converter fed BLDC motor at rated condition showing (a) continuous input inductor current (i_{Li1} , i_{Li2}) and (b) continuous intermediate capacitor voltages (v_{C1} , v_{C2}).
- Fig. 6.43 (a-b) Recorded performance of bridgeless PFC Cuk converter fed BLDC motor at rated condition showing (a) discontinuous output inductor current (i_{Lo1} , i_{Lo2}) and (b) its enlarged waveforms.
- Fig. 6.44 (a-b) Recorded performance of bridgeless PFC Cuk converter fed BLDC motor at rated condition showing (a) voltage (v_{sw1} , v_{sw2}) and current (i_{sw1} , i_{sw2}) stress on PFC converter switch and (b) its enlarged waveforms.
- Fig. 6.45 (a-b) Simulated dynamic performance of bridgeless PFC Cuk converter fed BLDC motor drive during (a) starting at DC link voltage of 50 V and (b) speed control at change in DC link voltage from 100 V to 150 V.
- Fig. 6.46 (a-b) Recorded dynamic performance of bridgeless PFC Cuk converter fed BLDC motor drive during (a) starting at DC link voltage of 50 V and (b) speed control at change in DC link voltage from 100 V to 150 V.
- Fig. 6.47 (a-b) Simulated dynamic performance of a bridgeless PFC Cuk converter fed BLDC motor drive during (a) step change in load from 0.4 Nm to 0.8 Nm and (b) step change in supply voltage from 270 V to 170 V.
- Fig. 6.48 (a-b) Recorded dynamic performance of a bridgeless PFC Cuk converter fed BLDC motor drive during (a) step change in load and (c) step change in supply voltage from 270 V to 200 V.
- Fig. 6.49 (a-b) Simulated harmonic spectrum of supply current at AC mains for a bridgeless PFC Cuk converter fed BLDC motor drive operating at rated condition with DC link voltage as (a) 200 V and (b) 50 V.
- Fig. 6.50 (a-f) Recorded power indices at AC mains for a bridgeless PFC Cuk converter fed BLDC motor drive operating at rated condition with DC link voltage as (a-c) 200 V and (d-f) 50 V.
- Fig. 6.51 (a-b) Simulated harmonic spectrum of supply current at AC mains for a bridgeless PFC Cuk converter fed BLDC motor drive operating at rated condition with supply voltage as (a) 90 V and (b) 270 V.
- Fig. 6.52 (a-f) Recorded power quality indices at AC mains for a bridgeless PFC Cuk converter fed BLDC motor drive operating at rated condition with supply voltage as (a-c) 90 V and (d-f) 270 V.

- Fig. 6.53 (a-b) Simulated steady state performance of a bridgeless PFC SEPIC fed BLDC motor at rated loading condition with DC link voltage as 200 V.
- Fig. 6.54 (a-b) Recorded steady state performance of a bridgeless PFC SEPIC fed BLDC motor at rated loading condition with DC link voltage as (a) 200 V and (b) 50 V.
- Fig. 6.55 (a-b) Recorded performance of bridgeless PFC SEPIC fed BLDC motor at rated condition showing (a) continuous input inductor current (i_{Li1} , i_{Li2}) and (b) continuous intermediate capacitor voltages (v_{C1} , v_{C2}).
- Fig. 6.56 (a-b) Recorded performance of bridgeless PFC Cuk converter fed BLDC motor at rated condition showing (a) discontinuous output inductor current (i_{Lo1} , i_{Lo2}) and (b) its enlarged waveforms.
- Fig. 6.57 (a-b) Recorded performance of bridgeless PFC SEPIC fed BLDC motor at rated condition showing (a) voltage (v_{sw1} , v_{sw2}) and current (i_{sw1} , i_{sw2}) stress on PFC converter switches and (b) its enlarged waveforms.
- Fig. 6.58 (a-b) Simulated dynamic performance of bridgeless PFC SEPIC fed BLDC motor drive during (a) starting at DC link voltage of 50 V and (b) speed control at change in DC link voltage from 100 V to 150 V.
- Fig. 6.59 (a-b) Recorded dynamic performance of bridgeless PFC SEPIC fed BLDC motor drive during (a) starting at DC link voltage of 50 V and (b) speed control at change in DC link voltage from 100 V to 150 V.
- Fig. 6.60 (a-b) Simulated dynamic performance of a bridgeless PFC SEPIC fed BLDC motor drive during (a) step change in load from 0.4 Nm to 0.8 Nm and (b) step change in supply voltage from 270 V to 170 V.
- Fig. 6.61 (a-b) Recorded dynamic performance of a bridgeless PFC SEPIC fed BLDC motor drive during (a) step change in load and (b) step change in supply voltage from 270 V to 200 V.
- Fig. 6.62 (a-b) Simulated harmonic spectrum of supply current at AC mains for a bridgeless PFC SEPIC fed BLDC motor drive operating at rated condition with DC link voltage as (a) 200 V and (b) 50 V.
- Fig. 6.63 (a-f) Recorded power indices at AC mains for a bridgeless PFC SEPIC fed BLDC motor drive operating at rated condition with DC link voltage as (a-c) 200 V and (d-f) 50 V.
- Fig. 6.64 (a-b) Simulated harmonic spectrum of supply current at AC mains for a bridgeless PFC SEPIC fed BLDC motor drive operating at rated condition with supply voltage as (a) 90 V and (b) 270 V.
- Fig. 6.65 (a-f) Recorded power quality indices at AC mains for a bridgeless PFC SEPIC fed BLDC motor drive operating at rated condition with supply voltage as (a-c) 90 V and (d-f) 270 V.

- Fig. 6.66 (a-b) Simulated steady state performance of a bridgeless PFC Zeta converter fed BLDC motor at rated loading condition with DC link voltage as 200 V.
- Fig. 6.67 (a-b) Simulated dynamic performance of bridgeless PFC Zeta converter fed BLDC motor drive during (a) starting at DC link voltage of 50 V and (b) speed control at change in DC link voltage from 100 V to 150 V.
- Fig. 6.68 (a-b) Simulated dynamic performance of a bridgeless PFC Zeta converter fed BLDC motor drive during (a) step change in load from 0.4 Nm to 0.8 Nm and (b) step change in supply voltage from 270 V to 170 V.
- Fig. 6.69 (a-b) Simulated harmonic spectrum of supply current at AC mains for a bridgeless PFC Zeta converter fed BLDC motor drive operating at rated condition with DC link voltage as (a) 200 V and (b) 50 V.
- Fig. 6.70 (a-b) Simulated harmonic spectrum of supply current at AC mains for a bridgeless PFC Zeta converter fed BLDC motor drive operating at rated condition with supply voltage as (a) 90 V and (b) 270 V.
- Fig. 6.71 (a-b) Simulated steady state performance of a bridgeless PFC Luo converter fed BLDC motor at rated loading condition with DC link voltage as 200 V.
- Fig. 6.72 (a-b) Recorded steady state performance of a bridgeless PFC Luo converter fed BLDC motor at rated loading condition with DC link voltage as (a) 200 V and (b) 50 V.
- Fig. 6.73 (a-b) Recorded performance of bridgeless PFC Luo converter fed BLDC motor at rated condition showing (a) inductor's currents (i_{Li1} , i_{Lo}) and intermediate capacitor voltage (v_{C1}) and (b) its enlarged waveforms.
- Fig. 6.74 (a-b) Recorded performance of bridgeless PFC Luo converter fed BLDC motor at rated condition showing (a) voltage (v_{sw1} , v_{sw2}) and current (i_{sw1} , i_{sw2}) stress on PFC converter switches and (b) its enlarged waveforms.
- Fig. 6.75 (a-b) Simulated dynamic performance of bridgeless PFC Luo converter fed BLDC motor drive during (a) starting at DC link voltage of 50 V and (b) speed control at change in DC link voltage from 100 V to 150 V.
- Fig. 6.76 (a-b) Recorded dynamic performance of bridgeless PFC Luo converter fed BLDC motor drive during (a) starting at DC link voltage of 50 V and (b) speed control at change in DC link voltage from 100 V to 150 V.
- Fig. 6.77 (a-b) Simulated dynamic performance of a bridgeless PFC Luo converter fed BLDC motor drive during (a) step change in load from 0.4 Nm to 0.8 Nm and (b) step change in supply voltage from 270 V to 170 V.
- Fig. 6.78 (a-b) Recorded dynamic performance of a bridgeless PFC Luo converter fed BLDC motor drive during (a) step change in load and (b) step change in supply voltage from 270 V to 200 V.

- Fig. 6.79 (a-b) Simulated harmonic spectrum of supply current at AC mains for a bridgeless PFC Luo converter fed BLDC motor drive operating at rated condition with DC link voltage as (a) 200 V and (b) 50 V.
- Fig. 6.80 (a-f) Recorded power indices at AC mains for a bridgeless PFC Luo converter fed BLDC motor drive operating at rated condition with DC link voltage as (a-c) 200 V and (d-f) 50 V.
- Fig. 6.81 (a-b) Simulated harmonic spectrum of supply current at AC mains for a bridgeless PFC Luo converter fed BLDC motor drive operating at rated condition with supply voltage as (a) 90 V and (b) 270 V.
- Fig. 6.82 (a-f) Recorded power quality indices at AC mains for a bridgeless PFC Luo converter fed BLDC motor drive operating at rated condition with supply voltage as (a-c) 90 V and (d-f) 270 V.
- Fig. 6.83 (a-b) Simulated steady state performance of a bridgeless PFC CSC converter fed BLDC motor at rated loading condition with DC link voltage as 200 V.
- Fig. 6.84 (a-b) Recorded steady state performance of a bridgeless PFC CSC converter fed BLDC motor at rated loading condition with DC link voltage as (a) 200 V and (b) 50 V.
- Fig. 6.85 (a-b) Recorded performance of bridgeless PFC CSC converter fed BLDC motor at rated condition showing (a) discontinuous inductor currents (i_{L1} , i_{L2}) and (b) continuous intermediate capacitor voltage (v_{C1} , v_{C2}).
- Fig. 6.86 (a-b) Recorded performance of bridgeless PFC CSC converter fed BLDC motor at rated condition showing (a) voltage (v_{sw1} , v_{sw2}) and current (i_{sw1} , i_{sw2}) stress on PFC converter switches and (b) its enlarged waveforms.
- Fig. 6.87 (a-b) Simulated dynamic performance of bridgeless PFC CSC converter fed BLDC motor drive during (a) starting at DC link voltage of 50 V and (b) speed control at change in DC link voltage from 100 V to 150 V.
- Fig. 6.88 (a-b) Recorded dynamic performance of bridgeless PFC CSC converter fed BLDC motor drive during (a) starting at DC link voltage of 50 V and (b) speed control at change in DC link voltage from 100 V to 150 V.
- Fig. 6.89 (a-b) Simulated dynamic performance of a bridgeless PFC CSC converter fed BLDC motor drive during (a) step change in load from 0.4 Nm to 0.8 Nm and (b) step change in supply voltage from 270 V to 170 V.
- Fig. 6.90 (a-b) Recorded dynamic performance of a bridgeless PFC CSC converter fed BLDC motor drive during (a) step change in load and (b) step change in supply voltage from 270 V to 200 V.
- Fig. 6.91 (a-b) Simulated harmonic spectrum of supply current at AC mains for a bridgeless PFC CSC converter fed BLDC motor drive operating at rated condition with DC link voltage as (a) 200 V and (b) 50 V.

- Fig. 6.92 (a-f) Recorded power indices at AC mains for a bridgeless PFC CSC converter fed BLDC motor drive operating at rated condition with DC link voltage as (a-c) 200 V and (d-f) 50 V.
- Fig. 6.93 (a-b) Simulated harmonic spectrum of supply current at AC mains for a bridgeless PFC CSC converter fed BLDC motor drive operating at rated condition with supply voltage as (a) 90 V and (b) 270 V.
- Fig. 6.94 (a-f) Recorded power quality indices at AC mains for a bridgeless PFC CSC converter fed BLDC motor drive operating at rated condition with supply voltage as (a-c) 90 V and (d-f) 270 V.
- Fig. 6.95 (a-b) Simulated steady state performance of a bridgeless PFC Sheppard-Taylor converter fed BLDC motor at rated condition with DC link voltage as 200 V.
- Fig. 6.96 (a-b) Simulated performance of bridgeless PFC Sheppard-Taylor converter fed BLDC motor drive during (a) starting at DC link voltage of 50 V and (b) speed control at change in DC link voltage from 100 V to 150 V.
- Fig. 6.97 (a-b) Simulated dynamic performance of a bridgeless PFC Sheppard-Taylor converter fed BLDC motor drive during (a) step change in load from 0.4 Nm to 0.8 Nm and (c) step change in supply voltage from 270 V to 170 V.
- Fig. 6.98 (a-b) Simulated harmonic spectrum of supply current at AC mains for a bridgeless PFC Sheppard-Taylor converter fed BLDC motor drive operating at rated condition with DC link voltage as (a) 200 V and (b) 50 V.
- Fig. 6.99 (a-b) Simulated harmonic spectrum of supply current at AC mains for a bridgeless PFC Sheppard-Taylor converter fed BLDC motor drive operating at rated condition with supply voltage as (a) 90 V and (b) 270 V.
- Fig. 6.100 (a-b) Simulated steady state performance of a bridgeless PFC switched-capacitor buck-boost converter fed BLDC motor at rated loading condition with DC link voltage as 200 V.
- Fig. 6.101 (a-b) Simulated performance of bridgeless PFC SC buck-boost converter fed BLDC motor drive during (a) starting at DC link voltage of 50 V and (b) speed control at change in DC link voltage from 100 V to 150 V.
- Fig. 6.102 (a-b) Simulated dynamic performance of a bridgeless PFC SC-buck-boost converter fed BLDC motor drive during (a) step change in load from 0.4 Nm to 0.8 Nm and (c) step change in supply voltage from 270 V to 170 V.
- Fig. 6.103 (a-b) Simulated harmonic spectrum of supply current at AC mains for a bridgeless PFC SC- buck-boost converter fed BLDC motor drive operating at rated condition with DC link voltage as (a) 200 V and (b) 50 V.
- Fig. 6.104 (a-b) Simulated harmonic spectrum of supply current at AC mains for a bridgeless PFC SC-buck-boost converter fed BLDC motor drive operating at rated condition with supply voltage as (a) 90 V and (b) 270 V.

- Fig. 7.1 Circuit configuration of PFC flyback converter fed BLDC motor drive.
- Fig. 7.2 Operation of PFC based flyback converter showing different modes of operations as (a) Mode-I, (b) Mode-II, and (c) Mode-III respectively and (d) the associated waveforms in a complete switching period.
- Fig. 7.3 Circuit configuration of PFC isolated-Cuk converter fed BLDC motor drive.
- Fig. 7.4 Operation of PFC based isolated-Cuk converter showing different modes of operations as (a) Mode-I, (b) Mode-II, and (c) Mode-III respectively and (d) the associated waveforms in a complete switching period.
- Fig. 7.5 Circuit configuration of PFC isolated SEPIC fed BLDC motor drive.
- Fig. 7.6 Operation of PFC based isolated-SEPIC showing different modes of operations as (a) Mode-I, (b) Mode-II, and (c) Mode-III respectively and (d) the associated waveforms in a complete switching period.
- Fig. 7.7 Circuit configuration of PFC isolated Zeta converter fed BLDC motor drive.
- Fig. 7.8 Operation of PFC based isolated-Zeta converter showing different modes of operations as (a) Mode-I, (b) Mode-II, and (c) Mode-III respectively and (d) the associated waveforms in a complete switching period.
- Fig. 7.9 Circuit configuration of PFC isolated Luo converter fed BLDC motor drive.
- Fig. 7.10 Operation of PFC based isolated-Luo converter showing different modes of operations as (a) Mode-I, (b) Mode-II, and (c) Mode-III respectively and (d) the associated waveforms in a complete switching period.
- Fig. 7.11 Circuit configuration of PFC isolated Sheppard-Taylor converter fed BLDC motor drive.
- Fig. 7.12 Operation of PFC based isolated-Sheppard Taylor converter showing different modes of operations as (a) Mode-I, (b) Mode-II, (c) Mode-III (d) Mode-IV and (e) Mode-IV respectively and (f) the associated waveforms in a complete switching period.
- Fig. 7.13 Control unit of a PFC converter operating in DCM with variable DC link voltage.
- Fig. 7.14 MATLAB/Simulink model of an Isolated PFC converter fed BLDC motor drive.
- Fig. 7.15 Simulated steady state performance of an isolated PFC flyback converter fed BLDC motor at rated loading condition with DC link voltage as 130 V.
- Fig. 7.16 Simulated dynamic performance of an isolated PFC flyback converter fed BLDC motor drive during (a) starting at DC link voltage of 50 V and (b) speed control at change in DC link voltage from 50 V to 100 V.

- Fig. 7.17 (a-b) Simulated dynamic performance of a an isolated PFC flyback converter fed BLDC motor drive during (a) step change in load from 0.5 Nm to 1 Nm and (b) step change in supply voltage from 270 V to 170 V.
- Fig. 7.18 (a-b) Simulated harmonic spectrum of supply current at AC mains for an isolated PFC flyback converter fed BLDC motor drive operating at rated condition with DC link voltage as (a) 130 V and (b) 50 V.
- Fig. 7.19 (a-b) Simulated harmonic spectrum of supply current at AC mains for an isolated PFC flyback converter fed BLDC motor drive operating at rated condition with supply voltage as (a) 90 V and (b) 270 V.
- Fig. 7.20 (a-b) Simulated steady state performance of an isolated PFC Cuk converter fed BLDC motor at rated loading condition with DC link voltage as 130 V.
- Fig. 7.21 (a-b) Recorded steady state performance of a PFC isolated-Cuk converter fed BLDC motor at rated loading condition with DC link voltage as (a) 130 V and (b) 50 V.
- Fig. 7.22 (a-b) Recorded performance of PFC isolated-Cuk converter fed BLDC motor at rated loading condition showing (a) input inductor current (i_{Li}) and (b) output inductor current (i_{Lo}).
- Fig. 7.23 (a-b) Recorded performance of PFC isolated-Cuk converter fed BLDC motor at rated condition showing (a) HFT primary (i_{HFTp}) and secondary (i_{HFTs}) current and (b) its enlarged waveforms.
- Fig. 7.24 (a-b) Recorded performance of PFC isolated-Cuk converter fed BLDC motor at rated condition showing (a) intermediate input capacitor voltage (v_{C1}) and (b) intermediate output capacitor voltage (v_{C2}).
- Fig. 7.25 (a-b) Recorded performance of PFC isolated-Cuk converter fed BLDC motor at rated condition showing (a) voltage and current stress on PFC converter switch (v_{sw} and i_{sw}) and (b) its enlarged waveforms.
- Fig. 7.26 (a-b) Simulated dynamic performance of an isolated PFC Cuk converter fed BLDC motor drive during (a) starting at DC link voltage of 50 V and (b) speed control at change in DC link voltage from 50 V to 100 V.
- Fig. 7.27 (a-b) Recorded dynamic performance of an isolated PFC Cuk converter fed BLDC motor drive during (a) starting at DC link voltage of 50 V and (b) speed control at change in DC link voltage from 50 V to 100 V.
- Fig. 7.28 (a-b) Simulated dynamic performance of a an isolated PFC Cuk converter fed BLDC motor drive during (a) step change in load from 0.5 Nm to 1 Nm and (b) step change in supply voltage from 270 V to 170 V.
- Fig. 7.29 (a-b) Recorded dynamic performance of a an isolated PFC Cuk converter fed BLDC motor drive during (a) step change in load from 0.5 Nm to 1 Nm and (b) step change in supply voltage from 270 V to 170 V.

- Fig. 7.30 (a-b) Simulated harmonic spectrum of supply current at AC mains for an isolated PFC Cuk converter fed BLDC motor drive operating at rated condition with DC link voltage as (a) 130 V and (b) 50 V.
- Fig. 7.31 (a-f) Recorded power indices at AC mains for a PFC isolated-Cuk converter fed BLDC motor drive operating at rated condition with DC link voltage as (a-c) 130 V and (d-f) 50 V.
- Fig. 7.32 (a-b) Simulated harmonic spectrum of supply current at AC mains for an isolated PFC Cuk converter fed BLDC motor drive operating at rated condition with supply voltage as (a) 90 V and (b) 270 V.
- Fig. 7.33 (a-f) Recorded power quality indices at AC mains for a PFC isolated-Cuk converter fed BLDC motor drive operating at rated condition with supply voltage as (a-c) 90 V and (d-f) 270 V.
- Fig. 7.34 Simulated steady state performance of an isolated PFC SEPIC fed BLDC motor at rated loading condition with DC link voltage as 130 V.
- Fig. 7.35 (a-b) Simulated dynamic performance of an isolated PFC SEPIC fed BLDC motor drive during (a) starting at DC link voltage of 50 V and (b) speed control at change in DC link voltage from 50 V to 100 V.
- Fig. 7.36 (a-b) Simulated dynamic performance of a an isolated PFC SEPIC fed BLDC motor drive during (a) step change in load from 0.5 Nm to 1 Nm and (b) step change in supply voltage from 270 V to 170 V.
- Fig. 7.37 (a-b) Simulated harmonic spectrum of supply current at AC mains for an isolated PFC SEPIC fed BLDC motor drive operating at rated condition with DC link voltage as (a) 130 V and (b) 50 V.
- Fig. 7.38 (a-b) Simulated harmonic spectrum of supply current at AC mains for an isolated PFC SEPIC fed BLDC motor drive operating at rated condition with supply voltage as (a) 90 V and (b) 270 V.
- Fig. 7.39 Simulated steady state performance of an isolated PFC Zeta converter fed BLDC motor at rated loading condition with DC link voltage as 130 V.
- Fig. 7.40 (a-b) Recorded steady state performance of a PFC isolated-Zeta converter fed BLDC motor at rated loading condition with DC link voltage as (a) 130 V and (b) 50 V.
- Fig. 7.41 (a-b) Recorded performance of PFC isolated-Zeta converter fed BLDC motor at rated condition showing (a) HFT primary (i_{HFTp}) and secondary (i_{HFTs}) current and (b) its enlarged waveforms.
- Fig. 7.42 (a-b) Recorded performance of PFC isolated-Zeta converter fed BLDC motor at rated condition showing (a) v_{CI} with v_s , i_s and V_{dc} and (b) its enlarged waveforms of v_{sw} and i_{sw} .

- Fig. 7.43 (a-b) Simulated dynamic performance of an isolated PFC Zeta converter fed BLDC motor drive during (a) starting at DC link voltage of 50 V and (b) speed control at change in DC link voltage from 50 V to 100 V.
- Fig. 7.44 (a-b) Recorded dynamic performance of an isolated PFC Zeta converter fed BLDC motor drive during (a) starting at DC link voltage of 50 V and (b) speed control at change in DC link voltage from 50 V to 100 V.
- Fig. 7.45 (a-b) Simulated dynamic performance of a an isolated PFC Zeta converter fed BLDC motor drive during (a) step change in load from 0.5 Nm to 1 Nm and (b) step change in supply voltage from 270 V to 170 V.
- Fig. 7.46 (a-b) Recorded dynamic performance of a an isolated PFC Zeta converter fed BLDC motor drive during (a) step change in load from 0.5 Nm to 1 Nm and (b) step change in supply voltage from 270 V to 170 V.
- Fig. 7.47 (a-b) Simulated harmonic spectrum of supply current at AC mains for an isolated PFC Zeta converter fed BLDC motor drive operating at rated condition with DC link voltage as (a) 130 V and (b) 50 V.
- Fig. 7.48 (a-f) Recorded power indices at AC mains for a PFC isolated-Zeta converter fed BLDC motor drive operating at rated condition with DC link voltage as (a-c) 130 V and (d-f) 50 V.
- Fig. 7.49 (a-b) Simulated harmonic spectrum of supply current at AC mains for an isolated PFC Zeta converter fed BLDC motor drive operating at rated condition with supply voltage as (a) 90 V and (b) 270 V.
- Fig. 7.50 (a-f) Recorded power quality indices at AC mains for a PFC isolated-Zeta converter fed BLDC motor drive operating at rated condition with supply voltage as (a-c) 90 V and (d-f) 270 V.
- Fig. 7.51 Simulated steady state performance of an isolated PFC Luo converter fed BLDC motor at rated loading condition with DC link voltage as 130 V.
- Fig. 7.52 (a-b) Simulated dynamic performance of an isolated PFC Luo converter fed BLDC motor drive during (a) starting at DC link voltage of 50 V and (b) speed control at change in DC link voltage from 50 V to 100 V.
- Fig. 7.53 (a-b) Simulated dynamic performance of a an isolated PFC Luo converter fed BLDC motor drive during (a) step change in load from 0.5 Nm to 1 Nm and (b) step change in supply voltage from 270 V to 170 V.
- Fig. 7.54 (a-b) Simulated harmonic spectrum of supply current at AC mains for an isolated PFC Luo converter fed BLDC motor drive operating at rated condition with DC link voltage as (a) 130 V and (b) 50 V.
- Fig. 7.55 (a-b) Simulated harmonic spectrum of supply current at AC mains for an isolated PFC Luo converter fed BLDC motor drive operating at rated condition with supply voltage as (a) 90 V and (b) 270 V.

- Fig. 7.56 (a-b) Simulated steady state performance of an isolated PFC Sheppard-Taylor converter fed BLDC motor at rated loading condition with DC link voltage as 130 V.
- Fig. 7.57 (a-b) Simulated performance of an isolated PFC Sheppard-Taylor converter fed BLDC motor drive during (a) starting at DC link voltage of 50 V and (b) speed control for change in DC link voltage from 50 V to 100 V.
- Fig. 7.58 (a-b) Simulated dynamic performance of a an isolated PFC Sheppard-Taylor converter fed BLDC motor drive during (a) step change in load from 0.5 Nm to 1 Nm and (c) step change in supply voltage from 270 V to 170 V.
- Fig. 7.59 (a-b) Simulated harmonic spectrum of supply current at AC mains for an isolated PFC Sheppard-Taylor converter fed BLDC motor drive operating at rated condition with DC link voltage as (a) 130 V and (b) 50 V.
- Fig. 7.60 (a-b) Simulated harmonic spectrum of supply current at AC mains for an isolated PFC Sheppard-Taylor converter fed BLDC motor drive operating at rated condition with supply voltage as (a) 90 V and (b) 270 V.
- Fig. 8.1 Circuit configuration of a bridgeless PFC isolated flyback converter fed BLDC motor drive.
- Fig. 8.2 (a-f) Operation of bridgeless PFC based flyback converter showing different modes of operations as (a) Mode P-I, (b) Mode P-II, (c) Mode P-III, (d) Mode N-I, (e) Mode N-II, (f) Mode N-III respectively.
- Fig. 8.3 (a-b) Operating waveforms of PFC based bridgeless flyback converter in (a) line cycle and (b) complete switching cycle.
- Fig. 8.4 Circuit configuration of a bridgeless PFC isolated-Cuk converter fed BLDC motor drive.
- Fig. 8.5 (a-f) Operation of bridgeless PFC isolated-Cuk converter showing different modes of operations as (a) Mode P-I, (b) Mode P-II, (c) Mode P-III, (d) Mode N-I, (e) Mode N-II, (f) Mode N-III respectively.
- Fig. 8.6 (a-b) Operating waveforms of PFC based bridgeless isolated-Cuk converter in (a) line cycle and (b) complete switching cycle.
- Fig. 8.7 Circuit configuration of a bridgeless PFC isolated SEPIC fed BLDC motor drive.
- Fig. 8.8 (a-f) Operation of bridgeless PFC isolated SEPIC showing different modes of operations as (a) Mode P-I, (b) Mode P-II, (c) Mode P-III, (d) Mode N-I, (e) Mode N-II, (f) Mode N-III respectively.
- Fig. 8.9 (a-b) Operating waveforms of PFC based bridgeless isolated-SEPIC during (a) line cycle and (b) complete switching cycle.
- Fig. 8.10 Circuit configuration of a bridgeless PFC isolated-Zeta converter fed BLDC motor drive.

- Fig. 8.11 (a-f) Operation of bridgeless PFC isolated-Zeta converter showing different modes of operations as (a) Mode P-I, (b) Mode P-II, (c) Mode P-III, (d) Mode N-I, (e) Mode N-II, (f) Mode N-III respectively.
- Fig. 8.12 (a-b) Operating waveforms of PFC based bridgeless isolated-Zeta Converter during (a) line cycle and (b) complete switching cycle.
- Fig. 8.13 Circuit configuration of a bridgeless PFC isolated-Luo converter fed BLDC motor drive.
- Fig. 8.14 (a-f) Operation of bridgeless PFC isolated-Luo converter showing different modes of operations as (a) Mode P-I, (b) Mode P-II, (c) Mode P-III, (d) Mode N-I, (e) Mode N-II, (f) Mode N-III respectively.
- Fig. 8.15 (a-b) Operating waveforms of PFC based bridgeless isolated-Luo Converter during (a) line cycle and (b) complete switching cycle.
- Fig. 8.16 Circuit configuration of a bridgeless PFC isolated-Sheppard-Taylor converter fed BLDC motor drive.
- Fig. 8.17 (a-e) Operation of bridgeless PFC isolated-Sheppard-Taylor converter showing different modes of operations as (a) Mode P-I, (b) Mode P-II, (c) Mode P-III, (d) Mode P-IV and (e) Mode P-V respectively.
- Fig. 8.18 (a-e) Operation of bridgeless PFC isolated-Sheppard-Taylor converter showing different modes of operations as (a) Mode N-I, (b) Mode N-II, (c) Mode N-III, (d) Mode N-IV and (e) Mode N-V respectively.
- Fig. 8.19 (a-b) Operating waveforms of PFC based bridgeless isolated-Sheppard-Taylor converter during (a) line cycle and (b) complete switching cycle.
- Fig. 8.20 Control unit of a PFC converter operating in DCM with variable DC link voltage.
- Fig. 8.21 MATLAB/Simulink model of an Isolated PFC converter fed BLDC motor drive.
- Fig. 8.22 (a-b) Simulated performance of a bridgeless isolated PFC Flyback converter fed BLDC motor at rated condition showing characteristics waveforms of (a) BLDC motor and (b) PFC converter.
- Fig. 8.23 (a-b) Simulated performance of a bridgeless isolated PFC flyback converter fed BLDC motor drive during (a) starting at DC link voltage of 50 V and (b) speed control for change in DC link voltage from 50 V to 100 V.
- Fig. 8.24 (a-b) Simulated dynamic performance of a bridgeless isolated PFC Flyback converter fed BLDC motor drive during (a) step change in load from 0.5 Nm to 1 Nm and (b) step change in supply voltage from 270 V to 170 V.
- Fig. 8.25 (a-b) Simulated harmonic spectrum of supply current at AC mains for a bridgeless isolated PFC flyback converter fed BLDC motor drive operating at rated condition with DC link voltage as (a) 130 V and (b) 50 V.

- Fig. 8.26 (a-b) Simulated harmonic spectrum of supply current at AC mains for a bridgeless isolated PFC flyback converter fed BLDC motor drive operating at rated condition with supply voltage as (a) 90 V and (b) 270 V.
- Fig. 8.27 (a-b) Simulated performance of a bridgeless isolated PFC Cuk converter fed BLDC motor at rated condition showing characteristics waveforms of (a) BLDC motor and (b) PFC converter.
- Fig. 8.28 (a-b) Recorded steady state performance of a bridgeless PFC isolated-Cuk converter fed BLDC motor at rated loading condition with DC link voltage as (a) 130 V and (b) 50 V.
- Fig. 8.29 (a-b) Recorded performance of bridgeless PFC isolated-Cuk converter fed BLDC motor at rated condition showing (a) input inductor currents (i_{Li1} , i_{Li2}) and (b) output inductor current (i_{Lo1} , i_{Lo2}).
- Fig. 8.30 (a-b) Recorded performance of bridgeless PFC isolated-Cuk converter fed BLDC motor at rated condition showing (a) HFT primary (i_{HFTp1}) and secondary (i_{HFTs1}) current and (b) its enlarged waveforms.
- Fig. 8.31 (a-b) Recorded performance of bridgeless PFC isolated-Cuk converter fed BLDC motor at rated condition showing (a) intermediate input capacitor voltage (v_{C11} , v_{C12}) and (b) intermediate output capacitor voltage (v_{C21} , v_{C22}).
- Fig. 8.32 (a-b) Recorded performance of bridgeless PFC isolated-Cuk converter fed BLDC motor at rated condition showing (a) voltage and current stress on PFC converter switch (v_{sw} and i_{sw}) and (b) its enlarged waveforms.
- Fig. 8.33 (a-b) Simulated performance of a bridgeless isolated PFC Cuk converter fed BLDC motor drive during (a) starting at DC link voltage of 50 V and (b) speed control for change in DC link voltage from 50 V to 100 V.
- Fig. 8.34 (a-b) Recorded dynamic performance of bridgeless isolated PFC Cuk converter fed BLDC motor drive during (a) starting at DC link voltage of 50 V and (b) speed control at change in DC link voltage from 50 V to 100 V.
- Fig. 8.35 (a-b) Simulated dynamic performance of a bridgeless isolated PFC Cuk converter fed BLDC motor drive during (a) step change in load from 0.5 Nm to 1 Nm and (c) step change in supply voltage from 270 V to 170 V.
- Fig. 8.36 (a-b) Recorded dynamic performance of bridgeless PFC isolated Cuk converter fed BLDC motor drive during (a) step change in load from 0.5 Nm to 1 Nm and (c) step change in supply voltage from 270 V to 170 V.
- Fig. 8.37 (a-b) Simulated harmonic spectrum of supply current at AC mains for a bridgeless isolated PFC Cuk converter fed BLDC motor drive operating at rated condition with DC link voltage as (a) 130 V and (b) 50 V.

- Fig. 8.38 (a-f) Recorded power indices at AC mains for a bridgeless PFC isolated Cuk converter fed BLDC motor drive operating at rated condition with DC link voltage as (a-c) 130 V and (d-f) 50 V.
- Fig. 8.39 (a-b) Simulated harmonic spectrum of supply current at AC mains for a bridgeless isolated PFC Cuk converter fed BLDC motor drive operating at rated condition with supply voltage as (a) 90 V and (b) 270 V.
- Fig. 8.40 (a-f) Recorded power quality indices at AC mains for a bridgeless PFC isolated Cuk converter fed BLDC motor drive operating at rated condition with supply voltage as (a-c) 90 V and (d-f) 270 V.
- Fig. 8.41 (a-b) Simulated performance of a bridgeless isolated PFC SEPIC fed BLDC motor at rated condition showing characteristics waveforms of (a) BLDC motor and (b) PFC converter.
- Fig. 8.42 (a-b) Simulated performance of a bridgeless isolated PFC SEPIC fed BLDC motor drive during (a) starting at DC link voltage of 50 V and (b) speed control for change in DC link voltage from 50 V to 100 V.
- Fig. 8.43 (a-b) Simulated dynamic performance of a bridgeless isolated PFC SEPIC fed BLDC motor drive during (a) step change in load from 0.5 Nm to 1 Nm and (b) step change in supply voltage from 270 V to 170 V.
- Fig. 8.44 (a-b) Simulated harmonic spectrum of supply current at AC mains for a bridgeless isolated PFC SEPIC fed BLDC motor drive operating at rated condition with DC link voltage as (a) 130 V and (b) 50 V.
- Fig. 8.45 (a-b) Simulated harmonic spectrum of supply current at AC mains for a bridgeless isolated PFC SEPIC fed BLDC motor drive operating at rated condition with supply voltage as (a) 90 V and (b) 270 V.
- Fig. 8.46 (a-b) Simulated performance of a bridgeless isolated PFC Zeta converter fed BLDC motor at rated condition showing characteristics waveforms of (a) BLDC motor and (b) PFC converter.
- Fig. 8.47 (a-b) Simulated performance of a bridgeless isolated PFC Zeta converter fed BLDC motor drive during (a) starting at DC link voltage of 50 V and (b) speed control for change in DC link voltage from 50 V to 100 V.
- Fig. 8.48 (a-b) Simulated dynamic performance of a bridgeless isolated PFC Zeta converter fed BLDC motor drive during (a) step change in load from 0.5 Nm to 1 Nm and (c) step change in supply voltage from 270 V to 170 V.
- Fig. 8.49 (a-b) Simulated harmonic spectrum of supply current at AC mains for a bridgeless isolated PFC Zeta converter fed BLDC motor drive operating at rated condition with DC link voltage as (a) 130 V and (b) 50 V.

- Fig. 8.50 (a-b) Simulated harmonic spectrum of supply current at AC mains for a bridgeless isolated PFC Zeta converter fed BLDC motor drive operating at rated condition with supply voltage as (a) 90 V and (b) 270 V.
- Fig. 8.51 (a-b) Simulated performance of a bridgeless isolated PFC Luo converter fed BLDC motor at rated condition showing characteristics waveforms of (a) BLDC motor and (b) PFC converter.
- Fig. 8.52 (a-b) Simulated performance of a bridgeless isolated PFC Luo converter fed BLDC motor drive during (a) starting at DC link voltage of 50 V and (b) speed control for change in DC link voltage from 50 V to 100 V.
- Fig. 8.53 (a-b) Simulated dynamic performance of a bridgeless isolated PFC Luo converter fed BLDC motor drive during (a) step change in load from 0.5 Nm to 1 Nm and (b) step change in supply voltage from 270 V to 170 V.
- Fig. 8.54 (a-b) Simulated harmonic spectrum of supply current at AC mains for a bridgeless isolated PFC Luo converter fed BLDC motor drive operating at rated condition with DC link voltage as (a) 130 V and (b) 50 V.
- Fig. 8.55 (a-b) Simulated harmonic spectrum of supply current at AC mains for a bridgeless isolated PFC Luo converter fed BLDC motor drive operating at rated condition with supply voltage as (a) 90 V and (b) 270 V.
- Fig. 8.56 (a-b) Simulated performance of a bridgeless isolated PFC Sheppard-Taylor converter fed BLDC motor at rated condition showing characteristics waveforms of (a) BLDC motor and (b) PFC converter.
- Fig. 8.57 (a-b) Simulated performance of a bridgeless isolated Sheppard-Taylor converter fed BLDC motor drive during (a) starting at DC link voltage of 50 V and (b) speed control for change in DC link voltage from 50 V to 100 V.
- Fig. 8.58 (a-b) Simulated dynamic performance of a bridgeless isolated PFC Sheppard-Taylor converter fed BLDC motor drive during step change in (a) load from 0.5 Nm to 1 Nm and (b) supply voltage from 270 V to 170 V.
- Fig. 8.59 (a-b) Simulated harmonic spectrum of supply current at AC mains for a bridgeless isolated PFC Sheppard-Taylor converter fed BLDC motor drive operating at rated condition with DC link voltage as (a) 130 V and (b) 50 V.
- Fig. 8.60 (a-b) Simulated harmonic spectrum of supply current at AC mains for a bridgeless isolated PFC Sheppard-Taylor converter fed BLDC motor drive operating at rated condition with supply voltage as (a) 90 V and (b) 270 V.
- Fig. 9.1 Circuit configuration of non-isolated PFC BIFRED converter fed BLDC motor drive.
- Fig. 9.2 (a-e) Operation of PFC based non-isolated BIFRED converter showing different modes of operations as (a) Mode-I, (b) Mode-II, (c) Mode-III, (d) Mode-IV and (e) the associated waveforms.

- Fig. 9.3 Circuit configuration of non-isolated PFC BIBRED converter fed BLDC motor drive.
- Fig. 9.4 Operation of PFC based non-isolated BIBRED converter showing different modes of operations as (a) Mode-I, (b) Mode-II, (c) Mode-III, (d) Mode-IV, (e) Mode-V and (f) the associated waveforms.
- Fig. 9.5 Circuit configuration of non-isolated PFC integrated buck-boost buck converter fed BLDC motor drive.
- Fig. 9.6 Operation of PFC based non-isolated integrated PFC buck-boost buck converter showing different modes of operations as (a) Mode-I, (b) Mode-II, (c) Mode-III, (d) Mode-IV and (e) the associated waveforms.
- Fig. 9.7 Circuit configuration of an isolated PFC BIFRED converter fed BLDC motor drive.
- Fig. 9.8 Operation of PFC based isolated PFC BIFRED converter showing different modes of operations as (a) Mode-I, (b) Mode-II, (c) Mode-III, (d) Mode-IV and (e) the associated waveforms.
- Fig. 9.9 Circuit configuration of an isolated PFC BIBRED converter fed BLDC motor drive.
- Fig. 9.10 Operation of PFC based isolated PFC BIBRED converter showing different modes of operations as (a) Mode-I, (b) Mode-II, (c) Mode-III, (d) Mode-IV and (e) the associated waveforms.
- Fig. 9.11 Circuit configuration of an isolated PFC boost-flyback SSIPP fed BLDC motor drive.
- Fig. 9.12 Operation of isolated PFC based boost-flyback SSIPP showing different modes of operations as (a) Mode-I, (b) Mode-II (c) Mode-III and (d) the associated waveforms.
- Fig. 9.13 Circuit configuration of an isolated PFC boost-forward SSIPP fed BLDC motor drive.
- Fig. 9.14 Operation of isolated PFC based boost-forward SSIPP showing different modes of operations as (a) Mode-I, (b) Mode-II, (c) Mode-III, (d) Mode-IV, e) Mode-V and (f) the associated waveforms.
- Fig. 9.15 Control unit of a PFC converter operating in DCM with variable DC link voltage.
- Fig. 9.16 MATLAB/Simulink model of an integrated and high quality rectifier fed BLDC motor drive.
- Fig. 9.17 Simulated steady state performance of a non-isolated PFC BIFRED converter fed BLDC motor at rated loading condition with DC link voltage as 200 V.

- Fig. 9.18 (a-b) Recorded steady state performance of a PFC non-isolated BIFRED converter fed BLDC motor at rated loading condition with DC link voltage as (a) 130 V and (b) 50 V.
- Fig. 9.19 (a-b) Recorded performance of PFC non-isolated BIFRED converter fed BLDC motor at rated condition showing (a) input and output inductor currents (i_{Li} , and i_{Lo}) and (b) intermediate capacitor voltage (v_{CI}).
- Fig. 9.20 (a-b) Recorded performance of PFC non-isolated BIFRED converter fed BLDC motor at rated condition showing (a) voltage and current stress on PFC converter switch (v_{sw} and i_{sw}) and (b) its enlarged waveforms.
- Fig. 9.21 (a-b) Simulated performance of non-isolated PFC BIFRED converter fed BLDC motor drive during (a) starting at DC link voltage of 50 V and (b) speed control at change in DC link voltage from 100 V to 150 V.
- Fig. 9.22 (a-b) Recorded dynamic performance of PFC non-isolated BIFRED converter fed BLDC motor drive during (a) starting at DC link voltage of 50 V and (b) speed control at change in DC link voltage from 100 V to 150 V.
- Fig. 9.23 (a-b) Simulated performance of a non-isolated PFC BIFRED converter fed BLDC motor drive during (a) step change in load from 0.4 Nm to 0.8 Nm and (b) step change in supply voltage from 270 V to 170 V.
- Fig. 9.24 (a-b) Recorded dynamic performance of PFC non-isolated BIFRED converter fed BLDC motor drive during (a) step change in load from 0.5 Nm to 1 Nm and (b) step change in supply voltage from 270 V to 170 V.
- Fig. 9.25 (a-b) Simulated harmonic spectrum of supply current at AC mains for a non-isolated PFC BIFRED converter fed BLDC motor drive operating at rated condition with DC link voltage as (a) 200 V and (b) 50 V.
- Fig. 9.26 (a-f) Recorded power indices at AC mains for a non-isolated PFC BIFRED converter fed BLDC motor drive operating at rated condition with DC link voltage as (a-c) 200 V and (d-f) 50 V.
- Fig. 9.27 (a-b) Simulated harmonic spectrum of supply current at AC mains for a non-isolated PFC BIFRED converter fed BLDC motor drive operating at rated condition with supply voltage as (a) 90 V and (b) 270 V.
- Fig. 9.28 (a-f) Recorded power quality indices at AC mains for a non-isolated PFC BIFRED converter fed BLDC motor drive operating at rated condition with supply voltage as (a-c) 100 V and (d-f) 270 V.
- Fig. 9.29 Simulated steady state performance of a non-isolated PFC BIBRED converter fed BLDC motor at rated loading condition with DC link voltage as 200 V.
- Fig. 9.30 (a-b) Simulated dynamic performance of non-isolated PFC BIBRED converter fed BLDC motor drive during (a) starting at DC link voltage of 50 V and (b) speed control at change in DC link voltage from 100 V to 150 V.

- Fig. 9.31 (a-b) Simulated dynamic performance of a non-isolated PFC BIBRED converter fed BLDC motor drive during (a) step change in load from 0.4 Nm to 0.8 Nm and (b) step change in supply voltage from 270 V to 170 V.
- Fig. 9.32 (a-b) Simulated harmonic spectrum of supply current at AC mains for a non-isolated PFC BIBRED converter fed BLDC motor drive operating at rated condition with DC link voltage as (a) 200 V and (b) 50 V.
- Fig. 9.33 (a-b) Simulated harmonic spectrum of supply current at AC mains for a non-isolated PFC BIBRED converter fed BLDC motor drive operating at rated condition with supply voltage as (a) 90 V and (b) 270 V.
- Fig. 9.34 Simulated steady state performance of a non-isolated PFC integrated buck-boost buck converter fed BLDC motor at rated loading condition with DC link voltage as 200 V.
- Fig. 9.35 (a-b) Simulated behavior of a PFC integrated buck-boost buck converter fed BLDC motor drive during (a) starting at DC link voltage of 50 V and (b) speed control at change in DC link voltage from 100 V to 150 V.
- Fig. 9.36 (a-b) Simulated dynamic performance of PFC integrated buck-boost buck converter fed BLDC motor drive during (a) step change in load from 0.4 Nm to 0.8 Nm and (b) step change in supply voltage from 270 V to 170 V.
- Fig. 9.37 (a-b) Simulated harmonic spectrum of supply current at AC mains for a PFC integrated buck-boost buck converter fed BLDC motor drive operating at rated condition with DC link voltage as (a) 200 V and (b) 50 V.
- Fig. 9.38 (a-b) Simulated harmonic spectrum of supply current at AC mains for a non-isolated PFC integrated buck-boost buck converter fed BLDC motor drive operating at rated condition with supply voltage as (a) 90 V and (b) 270 V.
- Fig. 9.39 Simulated steady state performance of an isolated PFC BIFRED converter fed BLDC motor at rated loading condition with DC link voltage as 130 V.
- Fig. 9.40 (a-b) Simulated dynamic performance of an isolated PFC BIFRED converter fed BLDC motor drive during (a) starting at DC link voltage of 50 V and (b) speed control at change in DC link voltage from 50 V to 100 V.
- Fig. 9.41 (a-b) Simulated dynamic performance of an isolated PFC BIFRED converter fed BLDC motor drive during (a) step change in load from 0.5 Nm to 1.0 Nm and (b) step change in supply voltage from 270 V to 170 V.
- Fig. 9.42 (a-b) Simulated harmonic spectrum of supply current at AC mains for an isolated PFC BIFRED converter fed BLDC motor drive operating at rated condition with DC link voltage as (a) 130 V and (b) 50 V.
- Fig. 9.43 (a-b) Simulated harmonic spectrum of supply current at AC mains for an isolated PFC BIFRED converter fed BLDC motor drive operating at rated condition with supply voltage as (a) 90 V and (b) 270 V.

- Fig. 9.44 Simulated steady state performance of an isolated PFC BIBRED converter fed BLDC motor at rated loading condition with DC link voltage as 130 V.
- Fig. 9.45 Simulated dynamic performance of an isolated PFC BIBRED converter fed BLDC motor drive during (a) starting at DC link voltage of 50 V and (b) speed control at change in DC link voltage from 50 V to 100 V.
- Fig. 9.46 Simulated dynamic performance of an isolated PFC BIBRED converter fed BLDC motor drive during (a) step change in load from 0.5 Nm to 1.0 Nm and (b) step change in supply voltage from 270 V to 170 V.
- Fig. 9.47 Simulated harmonic spectrum of supply current at AC mains for an isolated PFC BIBRED converter fed BLDC motor drive operating at rated condition with DC link voltage as (a) 130 V and (b) 50 V.
- Fig. 9.48 Simulated harmonic spectrum of supply current at AC mains for an isolated PFC BIBRED converter fed BLDC motor drive operating at rated condition with supply voltage as (a) 90 V and (b) 270 V.
- Fig. 9.49 Simulated steady state performance of an isolated PFC boost flyback SSIPP fed BLDC motor at rated loading condition with DC link voltage as 130 V.
- Fig. 9.50 Simulated dynamic performance of an isolated PFC boost flyback SSIPP fed BLDC motor drive during (a) starting at DC link voltage of 50 V and (b) speed control at change in DC link voltage from 50 V to 100 V.
- Fig. 9.51 Simulated dynamic performance of an isolated PFC boost flyback SSIPP converter fed BLDC motor drive during (a) step change in load from 0.5 Nm to 1.0 Nm and (b) step change in supply voltage from 270 V to 170 V.
- Fig. 9.52 Simulated harmonic spectrum of supply current at AC mains for an isolated PFC boost flyback SSIPP fed BLDC motor drive operating at rated condition with DC link voltage as (a) 130 V and (b) 50 V.
- Fig. 9.53 Simulated harmonic spectrum of supply current at AC mains for an isolated PFC boost flyback SSIPP fed BLDC motor drive operating at rated condition with supply voltage as (a) 90 V and (b) 270 V.
- Fig. 9.54 Simulated steady state performance of an isolated PFC boost forward SSIPP fed BLDC motor at rated loading condition with DC link voltage as 130 V.
- Fig. 9.55 Simulated dynamic performance of an isolated PFC boost forward SSIPP fed BLDC motor drive during (a) starting at DC link voltage of 50 V and (b) speed control at change in DC link voltage from 50 V to 100 V.
- Fig. 9.56 Simulated performance of an isolated PFC boost forward SSIPP converter fed BLDC motor drive during (a) step change in load from 0.5 Nm to 1 Nm and (b) step change in supply voltage from 270 V to 170 V.

- Fig. 9.57 (a-b) Simulated harmonic spectrum of supply current at AC mains for an isolated PFC boost forward SSIPP fed BLDC motor drive operating at rated condition with DC link voltage as (a) 130 V and (b) 50 V.
- Fig. 9.58 (a-b) Simulated harmonic spectrum of supply current at AC mains for an isolated PFC boost forward SSIPP fed BLDC motor drive operating at rated condition with supply voltage as (a) 90 V and (b) 270 V.
- Fig. 10.1 Circuit configuration of a non-isolated PFC Cuk converter fed sensorless BLDC motor drive.
- Fig. 10.2 Circuit configuration of a bridgeless non-isolated PFC Cuk converter fed sensorless BLDC motor drive.
- Fig. 10.3 Circuit configuration of an isolated PFC Cuk converter fed sensorless BLDC motor drive.
- Fig. 10.4 Circuit configuration of a bridgeless PFC isolated-Cuk converter fed sensorless BLDC motor drive.
- Fig. 10.5 Circuit configuration of a non-isolated BIFRED converter fed sensorless BLDC motor drive.
- Fig. 10.6 Circuit configurations for virtual Hall signals generation for BLDC motor.
- Fig. 10.7 Waveforms of the line back emf's and the corresponding actual Hall signals (H_a - H_c) and the required (estimated) Hall signals after the compensation.
- Fig. 10.8 Operation of hysteresis comparator with threshold voltage and the delay produced due to its operation.
- Fig. 10.9 Recorded delay of the virtual Hall signals with the actual Hall signals for different speeds.
- Fig. 10.10 Test results of terminal voltage with the actual and the virtual (estimated) Hall signals without phase-lead compensation.
- Fig. 10.11 Bode plot of the designed phase lead compensator.
- Fig. 10.12 Test results of terminal voltage with the actual and the virtual (estimated) Hall with phase lead compensation at rated conditions.
- Fig. 10.13 Recorded error in phase delay with and without compensation for different speeds.
- Fig. 10.14 Control scheme of proposed PFC based sensorless BLDC motor drive
- Fig. 10.15 Different modes of operation of a sensorless BLDC motor drive.
- Fig. 10.16 MATLAB/Simulink model of a PFC converter fed sensorless BLDC motor drive.

- Fig. 10.17 (a-b) Simulated steady state performance of a non-isolated PFC Cuk converter fed sensorless BLDC motor at rated loading condition with DC link voltage as (a) 200 V and (b) 50 V.
- Fig. 10.18 (a-b) Recorded steady state performance of a non-isolated PFC Cuk converter fed sensorless BLDC motor at rated loading condition with DC link voltage as (a) 200 V and (b) 50 V.
- Fig. 10.19 (a-b) Simulated performance of non-isolated PFC Cuk converter fed sensorless BLDC motor drive during (a) starting at DC link voltage of 50 V and (b) speed control at change in DC link voltage from 100 V to 150 V.
- Fig. 10.20 (a-b) Recorded performance of non-isolated PFC Cuk converter fed sensorless BLDC motor drive during (a) starting at DC link voltage of 50 V and (b) speed control at change in DC link voltage from 100 V to 150 V.
- Fig. 10.21 (a-b) Simulated dynamic performance of a non-isolated PFC Cuk converter fed sensorless BLDC motor drive during (a) step change in load from 0.4 Nm to 0.8 Nm and (b) step change in supply voltage from 270 V to 170 V.
- Fig. 10.22 (a-b) Recorded dynamic performance of a non-isolated PFC Cuk converter fed sensorless BLDC motor drive during (a) step change in load and (b) step change in supply voltage from 270 V to 200 V.
- Fig. 10.23 (a-b) Simulated harmonic spectrum of supply current at AC mains for a non-isolated PFC Cuk converter fed sensorless BLDC motor drive operating at rated condition with DC link voltage as (a) 200 V and (b) 50 V.
- Fig. 10.24 (a-f) Recorded power indices at AC mains for a non-isolated PFC Cuk converter fed sensorless BLDC motor drive operating at rated condition with DC link voltage as (a-c) 200 V and (d-f) 50 V.
- Fig. 10.25 (a-b) Simulated harmonic spectrum of supply current at AC mains for a non-isolated PFC Cuk converter fed sensorless BLDC motor drive operating at rated condition with supply voltage as (a) 90 V and (b) 270 V.
- Fig. 10.26 (a-f) Recorded power quality indices at AC mains for a non-isolated PFC Cuk converter fed sensorless BLDC motor drive operating at rated condition with supply voltage as (a-c) 90 V and (d-f) 270 V.
- Fig. 10.27 (a-b) Simulated steady state performance of a bridgeless non-isolated PFC Cuk converter fed BLDC motor at rated loading condition with DC link voltage as (a) 200 V and (b) 50 V.
- Fig. 10.28 (a-b) Recorded steady state performance of a bridgeless non-isolated PFC Cuk converter fed BLDC motor at rated loading condition with DC link voltage as (a) 200 V and (b) 50 V.

- Fig. 10.29 (a-b) Simulated performance of bridgeless PFC Cuk converter fed sensorless BLDC motor drive during (a) starting at DC link voltage of 50 V and (b) speed control at change in DC link voltage from 100 V to 150 V.
- Fig. 10.30 (a-b) Recorded performance of bridgeless PFC Cuk converter fed sensorless BLDC motor drive during (a) starting at DC link voltage of 50 V and (b) speed control at change in DC link voltage from 100 V to 150 V.
- Fig. 10.31 (a-b) Simulated dynamic performance of a bridgeless PFC Cuk converter fed sensorless BLDC motor drive during (a) step change in load from 0.4 Nm to 0.8 Nm and (b) step change in supply voltage from 270 V to 170 V.
- Fig. 10.32 (a-b) Recorded dynamic performance of a bridgeless PFC Cuk converter fed sensorless BLDC motor drive during (a) step change in load and (b) step change in supply voltage from 270 V to 200 V.
- Fig. 10.33 (a-b) Simulated harmonic spectrum of supply current at AC mains for a bridgeless PFC Cuk converter fed sensorless BLDC motor drive operating at rated condition with DC link voltage as (a) 200 V and (b) 50 V.
- Fig. 10.34 (a-f) Recorded power indices at AC mains for a bridgeless PFC Cuk converter fed sensorless BLDC motor drive operating at rated condition with DC link voltage as (a-c) 200 V and (d-f) 50 V.
- Fig. 10.35 (a-b) Simulated harmonic spectrum of supply current at AC mains for a bridgeless PFC Cuk converter fed sensorless BLDC motor drive operating at rated condition with supply voltage as (a) 90 V and (b) 270 V.
- Fig. 10.36 (a-f) Recorded power quality indices at AC mains for a bridgeless PFC Cuk converter fed sensorless BLDC motor drive operating at rated condition with supply voltage as (a-c) 90 V and (d-f) 270 V.
- Fig. 10.37 (a-b) Simulated steady state performance of an isolated PFC Cuk converter fed sensorless BLDC motor at rated loading condition with DC link voltage as (a) 200 V and (b) 50 V.
- Fig. 10.38 (a-b) Recorded steady state performance of a PFC isolated-Cuk converter fed sensorless BLDC motor at rated loading condition with DC link voltage as (a) 130 V and (b) 50 V.
- Fig. 10.39 (a-b) Simulated dynamic performance of an isolated PFC Cuk converter fed BLDC motor drive during (a) starting at DC link voltage of 50 V and (b) speed control at change in DC link voltage from 50 V to 100 V.
- Fig. 10.40 (a-b) Recorded performance of an isolated PFC Cuk converter fed sensorless BLDC motor drive during (a) starting at DC link voltage of 50 V and (b) speed control at change in DC link voltage from 50 V to 100 V.

- Fig. 10.41 (a-b) Simulated dynamic performance of a an isolated PFC Cuk converter fed sensorless BLDC motor drive during (a) step change in load from 0.5 Nm to 1 Nm and (b) step change in supply voltage from 270 V to 170 V.
- Fig. 10.42 (a-b) Recorded dynamic performance of a an isolated PFC Cuk converter fed sensorless BLDC motor drive during (a) step change in load from 0.5 Nm to 1 Nm and (b) step change in supply voltage from 270 V to 170 V.
- Fig. 10.43 (a-b) Simulated harmonic spectrum of supply current at AC mains for an isolated PFC Cuk converter fed BLDC motor drive operating at rated condition with DC link voltage as (a) 130 V and (b) 50 V.
- Fig. 10.44 (a-f) Recorded power indices at AC mains for a PFC isolated Cuk converter fed BLDC motor drive operating at rated condition with DC link voltage as (a-c) 130 V and (d-f) 50 V.
- Fig. 10.45 (a-b) Simulated harmonic spectrum of supply current at AC mains for an isolated PFC Cuk converter fed BLDC motor drive operating at rated condition with supply voltage as (a) 90 V and (b) 270 V.
- Fig. 10.46 (a-f) Recorded power quality indices at AC mains for a PFC isolated Cuk converter fed BLDC motor drive operating at rated condition with supply voltage as (a-c) 90 V and (d-f) 270 V.
- Fig. 10.47 (a-b) Simulated steady state performance of a bridgeless PFC isolated-Cuk converter fed sensorless BLDC motor at rated loading condition with DC link voltage as (a) 130 V and (b) 50 V.
- Fig. 10.48 (a-b) Recorded steady state performance of a bridgeless PFC isolated-Cuk converter fed sensorless BLDC motor at rated loading condition with DC link voltage as (a) 130 V and (b) 50 V.
- Fig. 10.49 (a-b) Simulated performance of a bridgeless isolated PFC Cuk converter fed BLDC motor drive during (a) starting at DC link voltage of 50 V and (b) speed control for change in DC link voltage from 50 V to 100 V.
- Fig. 10.50 (a-b) Recorded performance of bridgeless isolated Cuk converter fed sensorless BLDC motor drive during (a) starting at DC link voltage of 50 V and (b) speed control at change in DC link voltage from 50 V to 100 V.
- Fig. 10.51 (a-b) Simulated dynamic performance of a bridgeless isolated PFC Cuk converter fed BLDC motor drive during (a) step change in load from 0.5 Nm to 1 Nm and (b) step change in supply voltage from 270 V to 170 V.
- Fig.10.52 (a-b) Recorded performance of bridgeless PFC isolated Cuk converter fed sensorless BLDC motor drive during (a) step change in load from 0.5 Nm to 1 Nm and (b) step change in supply voltage from 270 V to 170 V.

- Fig. 10.53 (a-b) Simulated harmonic spectrum of supply current at AC mains for a bridgeless isolated PFC Cuk converter fed sensorless BLDC motor drive operating at rated condition with DC link voltage as (a) 130 V and (b) 50 V.
- Fig. 10.54 (a-f) Recorded power indices at AC mains for a bridgeless PFC isolated Cuk converter fed sensorless BLDC motor drive operating at rated condition with DC link voltage as (a-c) 130 V and (d-f) 50 V.
- Fig. 10.55 (a-b) Simulated harmonic spectrum of supply current at AC mains for a bridgeless isolated PFC Cuk converter fed sensorless BLDC motor drive operating at rated condition with supply voltage as (a) 90 V and (b) 270 V.
- Fig. 10.56 (a-f) Recorded power quality indices at AC mains for a bridgeless PFC isolated Cuk converter fed sensorless BLDC motor drive operating at rated condition with supply voltage as (a-c) 90 V and (d-f) 270 V.
- Fig. 10.57 (a-b) Recorded steady state performance of a PFC non-isolated BIFRED converter fed sensorless BLDC motor at rated loading condition with DC link voltage as (a) 200 V and (b) 50 V.
- Fig. 10.58 (a-b) Recorded steady state performance of a PFC non-isolated BIFRED converter fed BLDC motor at rated loading condition with DC link voltage as (a) 200 V and (b) 50 V.
- Fig. 10.59 (a-b) Simulated performance of non-isolated PFC BIFRED converter fed BLDC motor drive during (a) starting at DC link voltage of 50 V and (b) speed control at change in DC link voltage from 100 V to 150 V.
- Fig. 10.60 (a-b) Recorded performance of PFC non-isolated BIFRED converter fed sensorless BLDC motor drive during (a) starting at DC link voltage of 50 V and (b) speed control at change in DC link voltage from 100 V to 150 V.
- Fig. 10.61 (a-b) Simulated performance of a non-isolated PFC BIFRED converter fed sensorless BLDC motor drive during (a) step change in load from 0.4 Nm to 0.8 Nm and (b) step change in supply voltage from 270 V to 170 V.
- Fig. 10.62 (a-b) Recorded dynamic performance of PFC non-isolated BIFRED converter fed BLDC motor drive during (a) step change in load from 0.4 Nm to 0.8 Nm and (b) step change in supply voltage from 270 V to 170 V.
- Fig. 10.63 (a-b) Simulated harmonic spectrum of supply current at AC mains for a non-isolated PFC BIFRED converter fed BLDC motor drive operating at rated condition with DC link voltage as (a) 200 V and (b) 50 V.
- Fig. 10.64 (a-f) Recorded power indices at AC mains for a non-isolated PFC BIFRED converter fed BLDC motor drive operating at rated condition with DC link voltage as (a-c) 200 V and (d-f) 50 V.

Fig. 10.65 Simulated harmonic spectrum of supply current at AC mains for a non-isolated PFC BIFRED converter fed BLDC motor drive operating at rated condition with supply voltage as (a) 90 V and (b) 270 V.

Fig. 10.66 Recorded power quality indices at AC mains for a non-isolated PFC BIFRED converter fed BLDC motor drive operating at rated condition with supply voltage as (a-c) 93.3 V and (d-f) 267.1 V.

LIST OF TABLES

Table 4.1	Excited phase voltages and switching states based on Hall-effect position sensor signals
Table 4.2	Comparative analysis of proposed configuration with conventional schemes
Table 5.1	Design parameters of non-isolated PFC buck-boost converter
Table 5.2	Design parameters of non-isolated PFC Cuk converter
Table 5.3	Design parameters of non-isolated PFC SEPIC
Table 5.4	Design parameters of non-isolated PFC zeta converter
Table 5.5	Design parameters of non-isolated PFC Luo converter
Table 5.6	Design parameters of non-isolated PFC CSC converter
Table 5.7	Design parameters of non-isolated PFC Sheppard-Taylor converter
Table 5.8	Design parameters of non-isolated PFC switched-capacitor buck-boost converter
Table 5.9	Comparison of number of components in different configurations of non-isolated PFC converters
Table 5.10	Comparison of power quality indices in different configurations of non-isolated PFC converters (Simulated)
Table 5.11	Comparison of stress on PFC converter switches in different configurations of non-isolated PFC converters (Simulated)
Table 6.1	Design parameters of bridgeless non-isolated PFC buck-boost converter
Table 6.2	Design parameters of bridgeless non-isolated PFC Cuk converter
Table 6.3	Design parameters of bridgeless non-isolated PFC SEPIC
Table 6.4	Design parameters of bridgeless non-isolated PFC zeta converter
Table 6.5	Design parameters of bridgeless non-isolated PFC Luo converter
Table 6.6	Design parameters of bridgeless non-isolated PFC CSC converter
Table 6.7	Design parameters of bridgeless non-isolated PFC Sheppard-Taylor converter
Table 6.8	Design parameters of bridgeless non-isolated PFC switched-capacitor buck-boost converter
Table 6.9	Comparison of number of components in different configurations of bridgeless non-isolated PFC converters

Table 6.10	Comparison of power quality indices in different configurations of bridgeless non-isolated PFC converters (Simulated)
Table 6.11	Comparison of stress on PFC converter switches in different configurations of bridgeless non-isolated PFC converters (Simulated)
Table 7.1	Design parameters of isolated PFC flyback converter
Table 7.2	Design parameters of isolated PFC Cuk converter
Table 7.3	Design parameters of isolated PFC SEPIC
Table 7.4	Design parameters of isolated PFC zeta converter
Table 7.5	Design parameters of isolated PFC Luo converter
Table 7.6	Design parameters of isolated PFC Sheppard-Taylor converter
Table 7.7	Comparison of number of components in different configurations of isolated PFC converters
Table 7.8	Comparison of power quality indices in different configurations of isolated PFC converters (Simulated)
Table 7.9	Comparison of stress on PFC converter switches in different configurations of isolated PFC converters (Simulated)
Table 8.1	Design parameters of bridgeless isolated PFC flyback converter
Table 8.2	Design parameters of bridgeless isolated PFC Cuk converter
Table 8.3	Design parameters of bridgeless isolated PFC SEPIC
Table 8.4	Design parameters of bridgeless isolated PFC Zeta converter
Table 8.5	Design parameters of bridgeless isolated PFC Luo converter
Table 8.6	Design parameters of bridgeless isolated PFC Sheppard-Taylor converter
Table 8.7	Comparison of number of components in different configurations of bridgeless isolated PFC converters
Table 8.8	Comparison of power quality indices in different configurations of bridgeless isolated PFC converters (Simulated)
Table 8.9	Comparison of stress on PFC converter switches in different configurations of bridgeless isolated PFC converters (Simulated)
Table 9.1	Design parameters of non-isolated PFC BIFRED converter
Table 9.2	Design parameters of non-isolated PFC BIBRED converter
Table 9.3	Design parameters of non-isolated PFC integrated buck-boost buck converter
Table 9.4	Design parameters of isolated PFC BIFRED converter

- Table 9.5 Design parameters of isolated PFC BIBRED converter
- Table 9.6 Design parameters of isolated PFC Boost-Flyback SSIPP
- Table 9.7 Design parameters of isolated PFC Boost-Forward SSIPP
- Table 9.8 Comparison of number of components in different configurations of integrated and high quality rectifiers
- Table 9.9 Comparison of power quality indices and stress on PFC converter switches in different configurations of integrated and high quality rectifiers
- Table 9.10 Comparison of stress on PFC converter switches in different configurations of integrated and high quality rectifiers
- Table 10.1 Comparison of number of components in different configurations of PFC converters

LIST OF ABBREVIATIONS

AC	Alternating Current
BIBRED	Boost Integrated Buck Rectifier Energy Storage DC-DC Converter
BIFRED	Boost Integrated Flyback Rectifier Energy Storage DC-DC Converter
BL	Bridgeless
BLDC	Brushless DC Motor
CCM	Continuous Conduction Mode
CCVM	Continuous Capacitor Voltage Mode
CF	Crest Factor
CICM	Continuous Inductor Current Mode
CSI	Current Source Inverter
CSC	Canonical Switching Cell
DBR	Diode Bridge Rectifier
DC	Direct Current
DCM	Discontinuous Conduction Mode
DCVM	Discontinuous Capacitor Voltage Mode
DF	Distortion Factor
DICM	Discontinuous Inductor Current Mode
DPF	Displacement Power Factor
DSC	Digital Signal Controller
DSP	Digital Signal Processor / Digital Signal Processing
DTC	Direct Torque Control
EMI	Electro Magnetic Interference
FFS	Fundamental Frequency Switching
HFT	High Frequency Transformer
HVAC	Heating, Ventilation and Air Conditioning
IEC	International Electrotechnical Commission
IHQRR	Integrated High Quality Rectifiers Regulators

IPQC	Improved Power Quality Converters
PF	Power Factor
PFC	Power Factor Correction
PMBL	Permanent Magnet Brushless
PMBLDC	Permanent Magnet Brushless DC
PMSM	Permanent Magnet Synchronous Motor
PQ	Power Quality
PWM	Pulse Width Modulation
SC	Switched Capacitor
SEPIC	Single Ended Primary Inductance Converter
SSIPP	Single Stage, Single Phase Isolated Power Factor Corrected Power Supplies
ST	Sheppard-Taylor
THD	Total Harmonic Distortion
UPF	Unity Power factor
VOPFC	Variable Output Voltage Power Factor Correction
VSI	Voltage Source Inverter

LIST OF SYMBOLS

C_1, C_{11}, C_{12}	Capacitance of Input Side Intermediate Capacitors (F)
C_2, C_{21}, C_{22}	Capacitance of Output Side Intermediate Capacitors (F)
C_{1c}	Critical Capacitance of Input Side Intermediate Capacitors (F)
C_{2c}	Critical Capacitance of Output Side Intermediate Capacitors (F)
C_d	Capacitance DC Link Capacitor (F)
C_f	Capacitance of Filter Capacitor (F)
C_{fmax}	Maximum Capacitance of Filter Capacitor (F)
D	Duty Ratio
D_{max}	Maximum Duty Ratio
D_{min}	Minimum Duty Ratio
f_c	Filter Cut-off frequency (Hz)
f_L	Line frequency (Hz)
f_{sw}	Switching frequency (Hz)
I_{dc}	DC Link Current (A)
i_a, i_b, i_c	Phase currents of BLDC motor (A)
i_a^*, i_b^*, i_c^*	Reference Phase currents of BLDC motor (A)
i_{Li}, i_{Li1}, i_{Li2}	Input Side Inductor Current (A)
i_{Lo}, i_{Lo1}, i_{Lo2}	Output Side Inductor Current (A)
i_{sw}, i_{sw1}, i_{sw2}	PFC converter's Switch Current (A)
I_{s_peak}	Peak Value of Supply Current (A)
J	Moment of Inertia of BLDC Motor (Kg/m^2)
K_a	Torque (Current) Constant of BLDC motor (Nm/A)
K_{pi}	Proportional Gain of Current Controller
K_{ii}	Integral Gain of Current Controller
K_{pv}	Proportional Gain of Voltage Controller
K_{iv}	Integral Gain of Voltage Controller
$K_{p\omega}$	Proportional Gain of Speed Controller

$K_{i\omega}$	Integral Gain of Speed Controller
K_v	Voltage Constant of BLDC motor (V/krpm)
L_f	Filter Inductance (H)
L_i, L_{i1}, L_{i2}	Inductance of Input Side Inductor (H)
L_{ic}	Critical Inductance of Input Side Inductor (H)
L_m, L_{m1}, L_{m2}	Magnetizing Inductance of HFT (H)
L_{mc}	Critical Magnetizing Inductance of HFT (H)
L_{ph}	Per Phase Inductance of BLDC Motor (Ω)
L_o, L_{o1}, L_{o2}	Inductance of Output Side Inductor (H)
L_{oc}	Critical Inductance of Output Side Inductor (H)
L_s	Source Inductance (H)
m_{dv}	Modulating signals for Voltage PWM Generator
$m_{d\omega}$	Modulating signals for Speed PWM Generator
N	Speed of BLDC motor (rpm)
N_1	Number of Primary Turns of High Frequency Transformer
N_2	Number of Secondary Turns of High Frequency Transformer
N_2/N_1	Transformation ratio of High Frequency Transformer
P_i	Instantaneous Power (W)
P_{max}	Maximum Power (W)
P_{min}	Minimum Power (W)
P_{rated}	Rated Power of BLDC Motor (W)
R_L	Emulated Load Resistance (Ω)
R_{ph}	Per Phase Resistance of BLDC Motor (Ω)
T_e	Electromagnetic Torque of BLDC Motor (Nm)
T_e^*	Maximum Electromagnetic Torque of BLDC Motor (Nm)
T_{rated}	Rated Torque of BLDC Motor (Nm)
V_{cc}	Output of PI Controller (V)
V_{dc}	DC Link Voltage (V)
V_{dc}^*	Reference DC Link Voltage (V)

V_{dcm}	Rated DC Link Voltage of BLDC Motor (V)
V_{dcmax}	Maximum DC Link Voltage (V)
V_{dcmin}	Minimum DC Link Voltage (V)
v_G	Gate voltage
v_{in}	Input Voltage after DBR (V)
V_{in}	Average Value of Input Voltage after DBR (V)
V_m	Peak Value of Input Supply Voltage (V)
v_s	Supply Voltage (V)
V_{smin}	Minimum Supply Voltage (V)
V_{smax}	Maximum Supply Voltage (V)
V_{s-peak}	Peak Value of Supply Voltage (V)
v_{C1}, v_{C11}, v_{C12}	Input Side Intermediate Capacitor's Voltage (V)
v_{C2}, v_{C21}, v_{C22}	Output Side Intermediate Capacitor's Voltage (V)
v_{sw}, v_{sw1}, v_{sw2}	PFC converter's Switch Voltage (V)
ω	Speed of BLDC motor (rad/sec)
ω^*	Reference Speed of BLDC motor (rad/sec)
ω_e	Speed Error of BLDC motor (rad/sec)
ω_L	Line frequency (rad/sec)
ω_{rated}	Rated Speed of BLDC Motor (rad/sec)
$\Delta i_{Li}, \Delta i_{Li1}, \Delta i_{Li2}$	Ripple Current in Input Side Inductor (A)
$\Delta i_{Lo}, \Delta i_{Lo1}, \Delta i_{Lo2}$	Ripple Current in Output Side Inductor (A)
$\Delta v_{C1}, \Delta v_{C11}, \Delta v_{C12}$	Ripple Voltage across Input Side Intermediate Capacitor (V)
$\Delta v_{C2}, \Delta v_{C21}, \Delta v_{C22}$	Ripple Voltage across Output Side Intermediate Capacitor (V)
η	Percentage of Ripple Current in Input Inductor (%)
λ	Percentage of Ripple Current in Output Inductor (%)
γ	Percentage of Ripple Current in Magnetizing Inductance of HFT (%)
κ	Percentage of Ripple Voltage in Input Side Intermediate Capacitor (%)
ξ	Percentage of Ripple Voltage in Output Side Intermediate Capacitor (%)
δ	Percentage of Ripple Voltage in DC Link Capacitor (%)